Robust Optimization for SCED in AC-HVDC Power Systems

by

Milad Dehghani Filabadi

A thesis
presented to the University of Waterloo
in fulfillment of the
thesis requirement for the degree of
Master of Applied Sciences
in
Management Sciences

Waterloo, Ontario, Canada, 2019

Author's Declaration

I hereby declare that I am the sole author of this thesis. This is a true copy of the thesis, including any required final revisions, as accepted by my examiners.

I understand that my thesis may be made electronically available to the public.

Abstract

Wind power is a clean, renewable and low-carbon resource for power generation that has received increasing attention in power systems over the last few decades. There are two main challenges associated with the large-scale integration of wind power plants in the power system: i) the intermittent nature of wind power results in prediction errors that can greatly impact the system's operational security and reliability requirements, and ii) large-scale offshore wind farms are typically located far from onshore loads and require new developments in the transmission system of power grids, e.g., realization of mixed alternating current-high voltage direct current (AC-HVDC) power systems, which will introduce new reliability requirements to the system operator.

The security-constrained economic dispatch (SCED) problem deals with determining a power dispatch schedule, for all generating units, that minimizes the total operational cost, while taking into account system reliability requirements. Robust optimization (RO) has recently been used to tackle wind power uncertainty in the SCED problem. In the literature of RO, the budget of uncertainty was proposed to adjust the solution conservatism (robustness) such that higher budgets of uncertainty correspond to more conservative solutions. This thesis shows that the budget of uncertainty approach may not be meaningful for problems with RHS uncertainty since increasing the budget of uncertainty by more than a certain threshold may not always impact the level of conservatism. This thesis proposes a new tractable two-stage robust optimization model that effectively incorporates the budget of uncertainty in problems with RHS uncertainty, controls the level of conservatism, and provides meaningful insights on the trade-off between robustness and cost.

Furthermore, this thesis examines the applicability of the proposed robust approach for the SCED problem in mixed AC-HVDC power systems with large integration of wind power. The proposed robust SCED model considers the impact of wind power curtailment on the operational cost and reliability requirements of the system. Extensive numerical studies are provided to demonstrate the economic and operational advantages of the proposed robust SCED model in mixed AC-HVDC systems from five aspects: the effectiveness of the budget of uncertainty, robustness against uncertainty, contribution to real-time reliability, cost efficiency, and power transfer controllability.

Acknowledgements

My sincerest thanks and gratitude to my supervisors, Dr. Houra Mahmoudzadeh and Dr. Sahar Pirooz Azad, for their endless support, guidance, and encouragement throughout this masters. I am thrilled that I had this opportunity to work under their supervision in the last two years.

I would also like to thank my readers, Dr. Sibel Alumur Alev and Dr. Kankar Bhattacharya, for their time and valuable comments.

My best thanks to my friends Sagar, Mohab, Rahil, Miha, Shaghayegh, Kavitha, and Yashdeep for their valuable support and help during the last two years. I would also like to thank my labmate Kourosh for engaging in research discussion.

Finally, a very special thanks to my dearest friend, Yasamin, who always encouraged and supported me in many different ways.

Dedication

This thesis is dedicated to my family:

My parents, whom I will forever be indebted to. They unconditionally supported and encouraged me to pursue my dreams and curiosity.

My brother, who ignited a fire in my mind and taught me to "dream big" when I was 12. He always supported me to live a life that I wanted.

My sisters, who are my role models for perseverance and courage. They are the best and most supportive siblings I could hope for.

All I have and will accomplish are only possible due to their love and support.

Table of Contents

List of Figures

List of Tables

List of Abbreviations

AC alternating current 3, 4, 6, 13, 14, 33, 36–39, 44, 46, 47, 57, 62–64, 66–68, 70, 71

CF constant flows 66, 67

DC direct current 34–36, 39

DR downward reserve 57, 58, 61, 67, 68

ED economic dispatch 5, 6

FF flexible flows 66, 67

HVDC high voltage direct current 3, 4, 6, 13, 14, 33, 36, 38, 39, 44, 46, 47, 57, 62–64, 66–68, 70, 71

IDR inadequate downward reserve 57, 58, 60, 67, 68

IUR inadequate upward reserve 57, 58, 60, 67

RESs renewable energy sources 2, 4

RHS right-hand side 5, 7, 9–17, 19–21, 30, 32, 41, 70, 71

RO robust optimization 6, 7, 10, 15, 46, 50, 55, 57, 62, 64, 67, 70, 71

RTS reliability test system 47

RUR remaining upward reserve 57, 58, 61

SC security-constrained 4–6

SCED security-constrained economic dispatch 5–7, 12–14, 17, 33, 37, 39–42, 44, 46–48, 50, 52, 55, 57, 66, 70, 71

SCUC security-constrained unit commitment 6

SFF semi-flexible flows 66, 67

SP stochastic programming 5

UR upward reserve 57, 58, 60, 61

Nomenclature

The application-specific notations are as follows:

$\mathcal{A}$	Set of areas
$\mathcal{N}_a^I$	Set of internal buses in area a
$\mathcal{N}_a^C$	Set of boundary buses connected to area a
$\mathcal{G}_i$	Set of conventional generators at bus i
$\mathcal{K}_i$	Set of wind farms at bus i
$\mathcal{F}_a$	Set of internal transmission lines in area a
$\mathcal{T}$	Set of scheduling periods
C_g	Generation cost of conventional generator g
σ_k	Penalty cost of wind power curtailment of wind farm k
$D_{i,t}$	Load demand at bus i during period t

$\overline{F}_f/\underline{F}_f$	Upper/lower power flow limit of internal line f
$G^I_{f,i}$	Sensitivity coefficient of flow of internal line f to power injection at internal bus i
$\mathbf{H}$	Incidence matrix indicating the relationship between tie-line flows and boundary buses
$\underline{P}_g/\overline{P}_g$	Upper/lower power output limit of conventional generator g
$\hat{W}_{k,t}$	Predicted wind power output of wind farm k during period t
$\overline{W}_{k,t}/\underline{W}_{k,t}$	Upper/lower limit of the predicted wind power output of wind farm k during period t
$\tilde{W}_{k,t}$	Available wind power output of wind farm k during period t
U_g/D_g	Upward/downward ramping rate of conventional generator g
$R^u_{a,t}/R^d_{a,t}$	Upward/downward spinning reserve requirement for area a during period t
$\overline{L}_j/\underline{L}_j$	Upper/lower power flow limit of tie-line connected to boundary bus j
$\Gamma_{a,t}$	Budget of uncertainty of area a during period t
$\Gamma^E_{a,t}$	Effective Budget of uncertainty of area a during period t
$p_{g,t}$	Power output of conventional generator g during period t
$p^{ac}_{j,t}/p^{dc}_{j,t}$	AC/DC power injection at boundary bus j during period t
$\mathbf{p}^{dc}$	Vector of DC power injections at boundary buses

$\hat{s}_{k,t}$	Nominal admissible wind power of wind farm k during period t
$\overline{s}_{k,t}/\underline{s}_{k,t}$	Upper/lower limit of admissible wind power admissible interval of wind farm k during period t
$p^W_{k,t}$	Power output of wind farm k during period t
$r^+_{g,t}/r^-_{g,t}$	Upward/downward spinning reserve capacity of conventional generator g during period t
$\theta_{i,t}/v_{i,t}$	Voltage angle/magnitude of AC bus i during period t

Chapter 1

Introduction

1.1 Motivation: Power Dispatch under Uncertainty

Environmental concerns and commitments to fight climate change are changing the landscape of power systems across the world to shift power generation resources from fossil fuels to clean, reliable, low-carbon alternatives. For example, Ontario's climate leadership plan includes a long-term greenhouse gas emissions reduction target of 80% below the 1990 levels by 2050 (Di Placido et al., 2014). The integration of emission-free renewable energy sources (RESs) in the power system is a promising option and has received increasing attention. Among RESs, wind is one of the prominent sources of energy (Lopez et al., 2012), mainly due to its availability, zero emissions, costless fuel resource, and technological maturity (Morales-España, 2014).

Large-scale wind power integration poses various operational challenges to energy

systems. First, the uncertainties associated with the intermittent nature of wind, particularly forecast errors, can greatly impact the system's operational security and reliability requirements (Lund, 2010). Therefore one cannot accurately plan the power dispatch based on predicted data. Wind power uncertainty can directly or indirectly impact the system in various forms depending on the time horizon. In long-term planning (years to decades) and medium-term planning (month to years), wind power unpredictability adversely influences the system generation adequacy and management (Amelin, 2009). In short-term planning (hours to days), prediction errors may impact power output and reserve capacity which are determined based on available wind power forecast (Smith et al., 2007). Finally, in real-time planning (seconds to minutes), wind power volatility directly impacts the power system operation due to potentially violating the operational limits of the system.

Furthermore, large-scale wind farms (e.g., area 1 of Figure 1.1) are typically located far from load centers or are geographically distributed in different regions of a multi-area power system (Li et al., 2016a). In such systems, where distributed areas are connected via tie-lines, interregional power dispatches are crucial to: (i) fully utilize the wind power in a distributed multi-area system by exchanging the available wind power between neighboring areas and (ii) share reserve capacities among interconnected areas in case of sudden variations in wind power or load (Lieu et al., 1995).

Over the past century, alternating current (AC) technology has served as the primary technology for power transmission. However, the recent development of high voltage direct current (HVDC) transmission systems has become an attractive alternative due to its various advantages including: (i) improved controllability of transferred power, and (ii) reduced overall cost of transmission over long distances due to lower losses (Kim

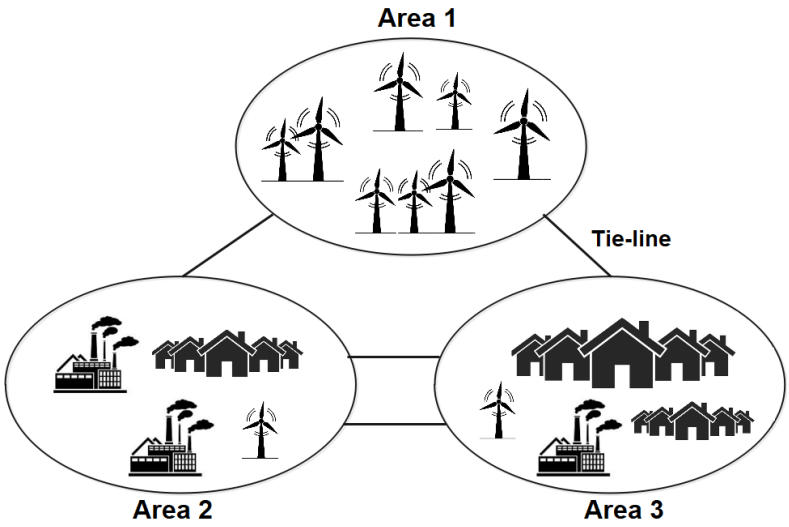

Figure 1.1: Abstract schematic of a multi-area power system

et al., 2009; Kundur et al., 1994). Converting the existing AC tie-lines of a multi-area system into HVDC tie-lines enables controllable and low-loss bulk power transfer among the various areas of a mixed AC-HVDC system.

Due to the fundamentally different operating characteristics of mixed AC-HVDC systems with RESs, as compared to AC systems with conventional generators, system safety and reliability faces various challenges. This thesis is motivated by the practical challenges for the integration of intermittent wind power generating units in mixed AC-HVDC power systems for short-term planning. In this thesis, a decision-making framework for power dispatch under uncertainty with an emphasis on wind power integration in mixed AC-HVDC systems is developed.

This chapter reviews the literature of security-constrained (SC) power dispatch problems. Next, the relevant background on decision-making under uncertainty is pre-

sented. Finally, the structure and contributions of this thesis are outlined.

1.2 Security-Constrained Power Dispatch Problems

In competitive electricity markets, a power dispatch with minimal cost is essential (Shahidehpour et al., 2003). The economic dispatch (ED) problem deals with determining the generation amount of generating units such that the required electric power is provided to all system loads (demand) at the lowest cost (Al Farsi et al., 2015). Reliability concerns have been one of the main focuses of researchers in power dispatch studies since 1960s (Billinton and Bollinger, 1968). Particularly, security-constrained (SC) dispatch problems are concerned with operational security and reliability of the system to mitigate the risk of a system failure under unforeseen contingencies (Frank and Rebennack, 2016). The security-constrained economic dispatch (SCED) is a branch of the ED problem where the objective is to find a power dispatch schedule that minimizes the total operational cost, while taking into account various operational constraints of generating resources, transmission lines, and reserves (Chowdhury and Rahman, 1990). In SC-based problems, wind power can be generated up to the available amount. Thus, the uncertainty associated with the available wind power is considered in the right-hand side (RHS) of constraints as an upper bound on wind power generation.

To tackle the wind uncertainty in such problems two main modeling approaches have been used in the literature. Stochastic programming (SP) is a technique that considers a probability distribution for the uncertain parameter in an optimization problem (Birge and Louveaux, 2011). SP was used by Wiget et al. (2014), Ahmadi-Khatir et al. (2013),

Wang et al. (2008), and Ruiz et al. (2009) to accommodate for wind power uncertainties in various power dispatch problems. The main drawback of this approach is that it requires the exact probability distribution of the uncertain parameter. Robust optimization (RO) (Bertsimas and Sim, 2004; Ben-Tal and Nemirovski, 1998) is an alternative tractable approach that does not rely on the probability distribution of the uncertain parameters, and instead, considers an uncertainty set that encapsulates all possible scenarios of an uncertain parameter. Then, it optimizes an objective function under the worst-case scenario of the uncertainty set to ensure problem feasibility under any other scenario of the uncertain parameter (Bertsimas and Sim, 2004).

The RO methodology has been extensively used to solve problems such as ED (Jabr, 2013; Xie et al., 2014; Wu et al., 2014; Li et al., 2015a, 2016a) and security-constrained unit commitment (SCUC) (Bertsimas et al., 2013; Ye and Li, 2016; Zhang et al., 2019) − which is a branch of the ED problem. However, only a few studies (e.g., Ding et al. (2016), Lu et al. (2018)) used an RO approach for solving the SCED problem that is the focus of this thesis. There are three main shortcomings associated with the existing RO models for SC dispatch problems in the literature: (i) A large number of studies assumed that wind power can be entirely absorbed in the power system (e.g., Lu et al. (2018); Ding et al. (2016)). However, when there is an excessive amount of wind power that cannot be absorbed by the system, the wind power should be "curtailed" to maintain the security of the power system and to have practically meaningful solutions; (ii) A number of studies lead to conservative robust solutions which may not be practical (e.g., Ding et al. (2016)); (iii) Most studies focus on single-area power systems or pure AC multi-area systems and do not consider the new advancements in multi-area power systems (e.g., Li et al. (2016a)), where HVDC transmission lines are used to transfer power from

offshore wind farms to onshore loads.

This thesis focuses on addressing the gaps in the literature of robust SCED optimization. In what follows, the relevant literature of RO is reviewed, and the gap in the literature of RO with RHS uncertainty is further elaborated on.

1.3 Robust Optimization

Soyster (1973) was the first to consider RO to tackle data uncertainty, and the theory was further refined in several studies (Ben-Tal and Nemirovski, 1998, 2002; Ben-Tal et al., 2009; Bertsimas and Sim, 2003; Bertsimas and Thiele, 2004). Recently, the applications of RO have been studied in various problems such as portfolio selection (e.g., Hassanzadeh et al. (2014)), network flows (e.g., Atamtürk and Zhang (2007)), inventory management (e.g., Ang et al. (2012)), radiation treatment planning (e.g., Chan et al. (2014)), as well as power dispatch problems (e.g., Li et al. (2016a)). See Bertsimas et al. (2011) and Gabrel et al. (2014) for a comprehensive review of other applications.

The main focus of this thesis is on the applications of RO in the SCED problem with RHS uncertainty. In what follows, two different classes of RO, i.e., "row-wise" and "column-wise" uncertainty, are introduced. Next, the relevant background on the budget of uncertainty and the potential challenges of having uncertainty in the RHS column of an optimization problem are presented.

1.3.1 Row-Wise Uncertainty versus Column-Wise Uncertainty

Ben-Tal and Nemirovski (1998, 2002) and El Ghaoui and Lebret (1997) studied "row-wise" uncertainty, i.e., where the rows of the constraint matrix belong to a given convex set, for different shapes of the uncertainty set (e.g., ellipsoid or polyhedral). In row-wise uncertainty, the complexity of the problem depends of the shape of the uncertainty set. For example, models with row-wise ellipsoidal and polyhedral uncertainty sets can be reformulated as conic quadratic and linear counterparts, respectively (Ben-Tal and Nemirovski, 1999; Bertsimas and Sim, 2003).

On the other hand, Soyster (1973) studied "column-wise" uncertainty, i.e., where the columns of the constraint matrix belong to a given uncertainty set, and proposed a linear model where columns $\mathbf{a}_i$'s of the constraint matrix belong to uncertainty sets $\mathcal{U}_i$ as follows:

$$\max_{\mathbf{x}} \quad \mathbf{c}^T\mathbf{x}, \tag{1.1a}$$

$$\text{s.t} \quad \sum_{i=1}^{n} x_i\mathbf{a}_i \leq \mathbf{b}, \qquad \forall \mathbf{a}_i \in \mathcal{U}_i, i = 1, ..., n \tag{1.1b}$$

$$\mathbf{x} \geq \mathbf{0}. \tag{1.1c}$$

It has been shown that the following linear problem can be used to guarantee the feasibility

of problem (1.1) under all scenarios.

$$\max_{\mathbf{x}} \quad \mathbf{c}^T\mathbf{x}, \tag{1.2a}$$

$$\text{s.t} \quad \sum_{i=1}^{n} x_i \mathbf{a}_i^* \leq \mathbf{b}, \tag{1.2b}$$

$$\mathbf{x} \geq \mathbf{0}. \tag{1.2c}$$

where $a_{ij}^* = \sup_{\mathbf{a}_i \in \mathcal{U}_j} (\mathbf{a}_i)_j$. The term sup indicates the supremum of a set and is the least upper bound of that set.

Column-wise uncertainty was further developed by Falk (1976) and Singh (1982). A special case of column-wise uncertainty is when uncertain parameters only appear in the RHS of a problem. However, addressing problems with uncertain RHS is more challenging. Specifically, Minoux (2008) considered problem (1.3) with an uncertain parameter $\tilde{\mathbf{b}}$ in the RHS.

$$\max_{\mathbf{x}} \quad \mathbf{c}^T\mathbf{x}, \tag{1.3a}$$

$$\text{s.t.} \quad \mathbf{x} \leq \tilde{\mathbf{b}}, \qquad \forall \tilde{\mathbf{b}} \in [\underline{\mathbf{b}}, \overline{\mathbf{b}}] \tag{1.3b}$$

$$\mathbf{x} \geq \mathbf{0}. \tag{1.3c}$$

Denoting $\boldsymbol{\alpha}$ as the vector of dual variables corresponding to constraint (1.3b), Minoux (2008) showed that the robust formulation of problem (1.3) can be derived through two possible formulations that are not necessarily equivalent. Specifically, formulation [**D1**] corresponds to the case where the worst-case of the uncertain parameter $\tilde{\mathbf{b}}$ is found, i.e., $\underline{\mathbf{b}} = \min_{\tilde{\mathbf{b}}}\{\tilde{\mathbf{b}}\}$, and then problem (1.3) is converted into an equivalent dual problem. However,

formulation [**D2**] corresponds to the the case where the equivalent dual reformulation of problem (1.3) is formulated first, and then the worst-case scenario of the dual problem is presented.

$$\begin{array}{lll} & [\mathbf{D1}] & [\mathbf{D2}] \\ \min\limits_{\boldsymbol{\alpha}} & \boldsymbol{\alpha}^T \underline{\mathbf{b}}, & \min\limits_{\boldsymbol{\alpha}} \max\limits_{\tilde{\mathbf{b}}} \quad \{\boldsymbol{\alpha}^T \tilde{\mathbf{b}}\}, \\ \text{s.t.} & \boldsymbol{\alpha}^T \geq \mathbf{c}, & \text{s.t.} \quad \boldsymbol{\alpha}^T \geq \mathbf{c}, \\ & \boldsymbol{\alpha}^T \geq \mathbf{0}. & \boldsymbol{\alpha}^T \geq \mathbf{0}. \end{array} \tag{1.4}$$

These problems may not lead to the same solutions as $\boldsymbol{\alpha}^T \underline{\mathbf{b}} \leq \max_{\tilde{\mathbf{b}}} \{\boldsymbol{\alpha}^T \tilde{\mathbf{b}}\}$, for $\boldsymbol{\alpha} \geq \mathbf{0}$ (Minoux, 2008). Therefore, the duality approach used for row-wise uncertainty cannot be directly applied to RHS uncertainty. Minoux (2012) and Ouorou (2016) further studied RHS uncertainty for specific shapes of uncertainty sets, such as polyhedral and ellipsoidal.

1.3.2 The Budget of Uncertainty

Since RO models seek to find a solution that is feasible under any realization of the uncertain parameter, they may lead to overly-conservative solutions (Bertsimas and Sim, 2004). For example, in Soyster's approach, in the worst-case scenario, every single entry of the constraint matrix is allowed to deviate from its nominal value. However, one could argue that the case in which all uncertain parameters take their absolute worst-case values is as unlikely as the case where all uncertain parameters are equal to their nominal values and have no deviation from what was predicted. This worst-case approach is therefore considered overly conservative in the literature.

Bertsimas and Sim (2004) later proposed the concept of "budget of uncertainty" to control the level of conservatism for problems with row-wise uncertainty. Assume that the uncertain parameter $\tilde{a}_{ij}$ can take any value within an uncertainty set $[\hat{a}_{ij} - \dot{a}_{ij}, \hat{a}_{ij} + \dot{a}_{ij}]$ where $\hat{a}_{ij}$ and $\dot{a}_{ij}$ are the nominal value and the error in estimating the nominal value, respectively. Parameter Γ_i is defined as the budget of uncertainty for each row i so that the maximum total scaled deviation, denoted as $z_{i,j}$, of all uncertain parameters within the same row i is limited to the budget of uncertainty Γ_i. The mathematical formulation of the budget of uncertainty for row i can be written as:

$$\begin{aligned} &\tilde{a}_{ij} = \hat{a}_{ij} + z_{ij}\dot{a}_{ij}, \qquad \forall i, j, \\ &|z_{ij}| \leq 1, \qquad \forall i, j, \qquad \sum_{j=1}^{n} |z_{ij}| \leq \Gamma_i \quad \forall i. \end{aligned} \tag{1.5}$$

Parameter Γ_i for row i can take values in $[0, |J_i|]$ where J_i is the set of coefficients that are subject to uncertainty in each row i. In particular, a zero budget, i.e., $\Gamma_i = 0$, corresponds to the nominal problem where the uncertain parameters do not deviate from the nominal values. If Γ_i increases, the solution becomes more conservative against uncertainty and results in a worse value of the objective function. Ultimately, a full budget, i.e., $\Gamma_i = |J_i|$, refers to the satisfaction of constraint i under all scenarios of the uncertainty set, which is equivalent to the worst-case approach.

The conventional budget of uncertainty approach proposed by Bertsimas and Sim (2004) may not be meaningful for some problems with uncertainty in the RHS. The intuition behind this issue is as follows: It is often expected to see a change in the objective value (level of conservatism) with a change in the budget; thus, the higher the budget,

the worse the objective value is expected to become. However, this behavior may not be observed explicitly with problems with RHS uncertainty. That is, deviating the value of the RHS parameters from their nominal value by more than a certain threshold may not have any further effect on the objective, simply because the corresponding constraint would become redundant. Therefore, any consideration of uncertainty beyond such threshold would be "ineffective" and the robust solution would remain unchanged regardless of the higher level of uncertainty considered. In this thesis, we refer to this phenomenon as "partially-ineffective budgets". The SCED problem with uncertainty in the available wind power falls into this general category.

1.4 Contributions

The specific contributions of this thesis are as follows:

- A modified column-wise budget of uncertainty approach is proposed for a class of problems with RHS uncertainty that have "partially-ineffective budgets". This approach converts the ineffective budgets of uncertainty into "effective" budgets and performs similar to the conventional budget approach defined for the row-wise uncertainty.

- A new tractable two-stage robust optimization model is developed to effectively incorporate the proposed budget approach. This thesis shows that the proposed two-stage approach accurately controls the level of robustness of the optimal solution without affecting the set of feasible solutions.

- The applicability of the proposed robust approach is demonstrated on the SCED problem in a mixed AC-HVDC multi-area system with large integration of wind power. While most studies do not consider the impact of wind power curtailment on system operation cost and reliability requirements, the proposed robust approach addresses wind power curtailments. Extensive numerical experiments are presented to examine the merits of the proposed robust approach in a mixed AC-HVDC system from five aspects: the effectiveness of the budget of uncertainty, robustness against uncertainty, contribution to real-time reliability, economic efficiency, and power transfer controllability.

1.5 Thesis Structure

The rest of this thesis is organized as follows. Chapter 2 discusses a new robust optimization approach for RHS uncertainty. In Chapter 3, the operational challenges of a mixed AC-HVDC system with wind power penetration are addressed and a robust formulation for the SCED problem is presented. In Chapter 4, the performance of the proposed approach is examined on various test systems and numerical results are discussed. Finally, Chapter 5 concludes the thesis and presents discussions for future research.

Chapter 2

A Robust Optimization Approach for Partially-Ineffective Uncertainty

Robust optimization (RO) with the budget of uncertainty has been mainly studied in problems with row-wise uncertainty, where the rows of the constraint matrix belong to a given convex set. However, there are several real-world applications − such as power dispatch problems, project management, scheduling, dynamic inventory management, and telecommunication problems − with right-hand side (RHS) uncertainty which is a special case of column-wise uncertainty. Addressing the budget of uncertainty in problems with uncertain RHS parameters is challenging since the budget may be partially-ineffective and may not meaningfully adjust the level of conservatism.

This chapter proposes an approach for RHS uncertainty when there are partially-ineffective uncertainty sets. The chapter is organized as follows: Section 2.1 defines a

general problem with uncertain RHS. In Section 2.2, admissible and effective uncertainty sets are introduced. Section 2.3 identifies an effective budget of uncertainty for such sets, and finally Section 2.4 proposes a two-stage robust optimization approach to tackle the challenges of RHS uncertainty with the budget of uncertainty.

2.1 Problem Definition

Consider problem [**M**] with uncertain parameter $\tilde{\mathbf{y}} \in \mathcal{U}$ as follows:

$$[\mathbf{M}]: \quad \min_{\mathbf{x},\mathbf{y}} \quad c_1(\mathbf{x}) + c_2(\mathbf{y}), \tag{2.1a}$$

$$\text{s.t.} \quad \mathbf{A}\mathbf{x} + \mathbf{B}\mathbf{y} \leq \mathbf{g}, \tag{2.1b}$$

$$\mathbf{y} \leq \tilde{\mathbf{y}}, \qquad \forall \tilde{\mathbf{y}} \in \mathcal{U} = [\underline{\mathbf{y}}, \overline{\mathbf{y}}] \tag{2.1c}$$

$$\mathbf{y}, \mathbf{x} \geq \mathbf{0}. \tag{2.1d}$$

Problem [**M**] corresponds to an optimization problem with two types of resources. The objective function consists of linear cost functions $c_1(\mathbf{x})$, i.e., the cost of using resource 1, and $c_2(\mathbf{y})$, i.e., the penalty for not utilizing resource 2, where each of decision variables $\mathbf{x}$ and $\mathbf{y}$ are vectors of size $m \times 1$. Let $c_2(\mathbf{y}) = \max_{\tilde{\mathbf{y}}} \mathbf{d}^T(\tilde{\mathbf{y}} - \mathbf{y})$ be the penalty for non-utilized resource 2 under the worst-case scenario. Constraint (2.1b) captures the limitations of the system on both $\mathbf{x}$ and $\mathbf{y}$, where matrices $\mathbf{A}$ and $\mathbf{B}$ are of size $n \times m$, and, for simplicity, consider $\mathbf{B} \geq \mathbf{0}$. In particular, $\mathbf{B} = \mathbf{0}$ corresponds to the upper limit of vector $\mathbf{x}$. The objective function maximizes the amount of resource 2 used while considering the uncertainty in its available amount, as shown in the RHS of constraint (2.1c). In

particular, model [**M**] can be used for the SCED problem where vectors $\mathbf{x}$ and $\mathbf{y}$ correspond to the power generation of conventional generators and wind power plants, respectively. Thus, $c_2(\mathbf{y})$ corresponds to the penalty for wind power curtailment, and the uncertainty of available wind power is considered in the RHS of constraint (2.1c).

Following the concept of the budget of uncertainty proposed by Bertsimas and Sim (2004), consider the uncertainty set $\mathcal{U}^B$ with budget Γ as follows:

$$\mathcal{U}^B := \Big\{ \tilde{\mathbf{y}} \in \mathcal{R}^m : \quad \tilde{\mathbf{y}} = \hat{\mathbf{y}} + \mathbf{z} \odot (\overline{\mathbf{y}} - \hat{\mathbf{y}}), \quad \sum_{i=1}^{m} z_i \leq \Gamma, \quad \mathbf{0} \leq \mathbf{z} \leq \mathbf{1}. \Big\}, \tag{2.2}$$

where $\hat{\mathbf{y}}$ is the nominal value of the uncertain parameter and the worst-case realization of $\tilde{\mathbf{y}}$ always occurs within $[\hat{\mathbf{y}}, \overline{\mathbf{y}}]$ - this point is later proved in Proposition 4.

In (2.2), operator $\odot$ is the "Hadamard Product" (Horn, 1990) and is used throughout this chapter for expressing element-wise multiplication of vectors with the same dimension where

$$\mathbf{z} \odot (\overline{\mathbf{y}} - \hat{\mathbf{y}}) = \begin{pmatrix} z_1 \\ \vdots \\ z_m \end{pmatrix} \odot \begin{pmatrix} \overline{y}_1 - \hat{y}_1 \\ \vdots \\ \overline{y}_m - \hat{y}_m \end{pmatrix} = \begin{pmatrix} z_1(\overline{y}_1 - \hat{y}_1) \\ \vdots \\ z_m(\overline{y}_m - \hat{y}_m) \end{pmatrix}.$$

Incorporating $\mathcal{U}^B$ in formulation [**M**], the following formulation is obtained:

$$\min_{\mathbf{x},\mathbf{y},\mathbf{z}} \quad c_1(\mathbf{x}) + c_2(\mathbf{y}), \tag{2.3a}$$

$$\text{s.t} \quad \mathbf{A}\mathbf{x} + \mathbf{B}\mathbf{y} \leq \mathbf{g}, \tag{2.3b}$$

$$\mathbf{y} \leq \hat{\mathbf{y}} + \mathbf{z} \odot (\overline{\mathbf{y}} - \hat{\mathbf{y}}), \tag{2.3c}$$

$$\sum_{i=1}^{m} z_i \leq \Gamma, \tag{2.3d}$$

$$\mathbf{0} \leq \mathbf{z} \leq \mathbf{1}, \tag{2.3e}$$

$$\mathbf{x}, \mathbf{y} \geq \mathbf{0}. \tag{2.3f}$$

Based on constraints (2.3b) and (2.3c), two upper bounds can be written for $\mathbf{A}\mathbf{x} + \mathbf{B}\mathbf{y}$ as follows:

$$\mathbf{A}\mathbf{x} + \mathbf{B}\mathbf{y} \leq \mathbf{g}, \tag{2.4a}$$

$$\mathbf{A}\mathbf{x} + \mathbf{B}\mathbf{y} \leq \mathbf{A}\mathbf{x} + \mathbf{B}\Big(\hat{\mathbf{y}} + \mathbf{z} \odot (\overline{\mathbf{y}} - \hat{\mathbf{y}})\Big). \tag{2.4b}$$

Depending on the value of $\mathbf{z}$, one of the constraints (2.4a) and (2.4b) would become redundant and would not impact the solution. Consider a feasible $\mathbf{z}^0$ such that (2.4a) is binding and $\mathbf{g} = \mathbf{A}\mathbf{x} + \mathbf{B}\big(\hat{\mathbf{y}} + \mathbf{z}^0 \odot (\overline{\mathbf{y}} - \hat{\mathbf{y}})\big)$. Denote the budget and the robust solution corresponding to $\mathbf{z}^0$ as Γ^0 and $\mathbf{y}^0$, respectively. When $\mathbf{B} > 0$, $\forall \mathbf{z}^1 \in (\mathbf{z}^0, \mathbf{1}]$, it can be shown that $\mathbf{g} < \mathbf{A}\mathbf{x} + \mathbf{B}\big(\hat{\mathbf{y}} + \mathbf{z}^1 \odot (\overline{\mathbf{y}} - \hat{\mathbf{y}})\big)$ and hence constraint (2.4b) becomes redundant. Let Γ^1 and $\mathbf{y}^1$ be the budget and the robust solution corresponding to $\mathbf{z}^1$, respectively; For $\Gamma^1 > \Gamma^0$ (as $\mathbf{z}^1 > \mathbf{z}^0$), $\mathbf{y}^1 = \mathbf{y}^0$ since the additional budget does not have any further impact on the solution. Thus, even though there is a penalty in the objective function for

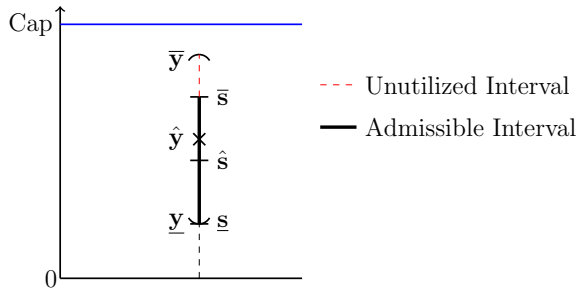

Figure 2.1: Comparison between uncertainty set $[\underline{\mathbf{y}}, \overline{\mathbf{y}}]$, admissible interval $[\underline{\mathbf{s}}, \overline{\mathbf{s}}]$, and effective interval $[\hat{\mathbf{s}}, \overline{\mathbf{s}}]$.

underutilization of resource 2, constraint (2.4a) may not allow $\mathcal{U} = [\underline{\mathbf{y}}, \overline{\mathbf{y}}]$ to be entirely utilized. In this thesis, the value of $\Gamma^1 - \Gamma^0$ is called the "ineffective" budget of uncertainty and can be calculated as $\sum_{i=1}^{m}(z_i{}^1 - z_i{}^0)$.

The following section introduces "admissible" and "effective" uncertainty sets that can be entirely utilized.

2.2 Admissible and Effective Uncertainty Sets

This section introduces "admissible" and "effective" intervals for RHS uncertainty. The admissible interval $[\underline{\mathbf{s}}, \overline{\mathbf{s}}]$ is defined as a subset of $[\mathbf{0}, \overline{\mathbf{y}}]$ such that for any solution $\mathbf{y} \in [\underline{\mathbf{s}}, \overline{\mathbf{s}}]$ the problem is feasible. The effective interval $[\hat{\mathbf{s}}, \overline{\mathbf{s}}]$ is a subset of the admissible interval within which the worst-case scenario of the admissible interval always occurs. Fig. 2.1 shows the admissible and effective intervals. In what follows, an optimization problem is first proposed to obtain the admissible interval. Next, the effective interval is derived accordingly.

2.2.1 Admissible Interval

The admissible interval $[\underline{\mathbf{s}}, \bar{\mathbf{s}}]$ is within interval $[\mathbf{0}, \overline{\mathbf{y}}]$, and may partially or entirely lay outside of the uncertainty set $[\underline{\mathbf{y}}, \overline{\mathbf{y}}]$ since the RHS parameters might not be fully utilized. Thus:

$$\bar{\mathbf{s}} \leq \overline{\mathbf{y}}, \tag{2.5a}$$

$$\underline{\mathbf{s}} \leq \underline{\mathbf{y}}, \tag{2.5b}$$

where $\bar{\mathbf{s}} = \overline{\mathbf{y}}$ means that the RHS can be fully utilized and the entire uncertainty set is admissible. Proposition 1 demonstrates how to identify whether a given interval $[\underline{\mathbf{s}}, \bar{\mathbf{s}}]$ is entirely admissible. Remark 1 further explains how to find the largest possible such interval that is as close as possible to the uncertainty set $\mathcal{U} = [\underline{\mathbf{y}}, \overline{\mathbf{y}}]$.

Proposition 1. *Any solution* $\mathbf{y} \in [\underline{\mathbf{s}}, \bar{\mathbf{s}}]$ *satisfies constraint* (2.1b) *of formulation* [**M**] *under any scenario of the uncertainty set if* $\underline{\mathbf{s}}$ *and* $\bar{\mathbf{s}}$ *meet the following conditions:*

$$\mathbf{A}\mathbf{x} + \mathbf{B}\underline{\mathbf{s}} + \boldsymbol{\alpha} \leq \mathbf{g}, \tag{2.6a}$$

$$\boldsymbol{\alpha} \geq \mathbf{B}(\bar{\mathbf{s}} - \underline{\mathbf{s}}), \tag{2.6b}$$

$$\boldsymbol{\alpha} \geq \mathbf{0}. \tag{2.6c}$$

Proof. Variable $\mathbf{y} \in [\underline{\mathbf{s}}, \bar{\mathbf{s}}]$ can be written as $\underline{\mathbf{s}} + \mathbf{r} \odot (\bar{\mathbf{s}} - \underline{\mathbf{s}})$, where $\mathbf{0} \leq \mathbf{r} \leq \mathbf{1}$. Thus, constraint (2.1b) is reformulated as $\mathbf{A}\mathbf{x} + \mathbf{B}\mathbf{y} \leq \mathbf{A}\mathbf{x} + \mathbf{B}(\underline{\mathbf{s}} + \mathbf{r} \odot (\bar{\mathbf{s}} - \underline{\mathbf{s}})) \leq \mathbf{g}$. To meet this constraint under its worst-case scenario, the following constrains should be satisfied:

$$\mathbf{A}\mathbf{x} + \mathbf{B}\mathbf{y} \leq \mathbf{A}\mathbf{x} + \boldsymbol{\beta}(\mathbf{r}) \leq \mathbf{g}, \tag{2.7}$$

where

$$\boldsymbol{\beta}(\mathbf{r}) = \max_{\mathbf{r}} \quad \mathbf{B}\Big(\underline{\mathbf{s}} + \mathbf{r} \odot (\overline{\mathbf{s}} - \underline{\mathbf{s}})\Big), \tag{2.8a}$$

$$\text{s.t.} \quad \mathbf{0} \leq \mathbf{r} \leq \mathbf{1}. \tag{2.8b}$$

Considering $\boldsymbol{\alpha}$ as the dual vector for constraint (2.8b) and replacing the dual of problem (2.8) into (2.7), formulation (2.6) can be recovered. □

Remark 1. *The following optimization problem finds the largest admissible interval* $[\underline{\mathbf{s}}, \overline{\mathbf{s}}]$ *that has the smallest distance from the uncertainty set* $\mathcal{U} = [\underline{\mathbf{y}}, \overline{\mathbf{y}}]$.

$$\min_{\underline{\mathbf{s}}, \overline{\mathbf{s}}, \boldsymbol{\alpha}, \mathbf{x}} \quad (\overline{\mathbf{y}} - \overline{\mathbf{s}}) + (\underline{\mathbf{y}} - \underline{\mathbf{s}}), \tag{2.9a}$$

$$\text{s.t.} \quad \mathbf{A}\mathbf{x} + \mathbf{B}\underline{\mathbf{s}} + \boldsymbol{\alpha} \leq \mathbf{g}, \tag{2.9b}$$

$$\boldsymbol{\alpha} \geq \mathbf{B}(\overline{\mathbf{s}} - \underline{\mathbf{s}}), \tag{2.9c}$$

$$\overline{\mathbf{s}} \leq \overline{\mathbf{y}}, \tag{2.9d}$$

$$\underline{\mathbf{s}} \leq \underline{\mathbf{y}}, \tag{2.9e}$$

$$\mathbf{x}, \underline{\mathbf{s}}, \overline{\mathbf{s}}, \boldsymbol{\alpha} \geq \mathbf{0}. \tag{2.9f}$$

Proof. As shown in Proposition 1, constraints (2.9b), (2.9c), and $\boldsymbol{\alpha} \geq \mathbf{0}$ in (2.9f) identify whether a given interval $[\underline{\mathbf{s}}, \overline{\mathbf{s}}]$ is admissible. Constraints (2.9d) and (2.9e) demonstrate that the admissible interval may lay outside of the uncertainty set since the RHS parameters might not be fully utilized. Given that the objective function (2.9a) minimizes the gap between $[\underline{\mathbf{y}}, \overline{\mathbf{y}}]$ and $[\underline{\mathbf{s}}, \overline{\mathbf{s}}]$, formulation (2.9) always obtains the largest possible admissible interval. □

Proposition 2. *The admissible interval* $[\underline{\mathbf{s}}, \overline{\mathbf{s}}]$ *can always be categorized as one of the following four cases:*

a) $\underline{\mathbf{s}} = \underline{\mathbf{y}}$ *and* $\overline{\mathbf{s}} = \overline{\mathbf{y}}$

b) $\underline{\mathbf{s}} = \underline{\mathbf{y}}$ *and* $\hat{\mathbf{y}} \leq \overline{\mathbf{s}} < \overline{\mathbf{y}}$

c) $\underline{\mathbf{s}} = \underline{\mathbf{y}}$ *and* $\underline{\mathbf{y}} < \overline{\mathbf{s}} < \hat{\mathbf{y}}$

d) $\underline{\mathbf{s}} = \overline{\mathbf{s}} \leq \underline{\mathbf{y}}$

Proof. For any feasible solution of problem (2.9), $\exists \boldsymbol{\alpha} \geq \mathbf{0}$, such that $\boldsymbol{\alpha} \geq \mathbf{B}(\overline{\mathbf{s}} - \underline{\mathbf{s}})$. By assumption, $\mathbf{B} \geq \mathbf{0}$. If $\mathbf{B} = \mathbf{0}$, constraint (2.9c) would become redundant since $\mathbf{B}(\underline{\mathbf{s}} - \overline{\mathbf{s}}) = \mathbf{0}$. Constraint (2.9b) is also independent on $\underline{\mathbf{s}}$ since $\mathbf{B}\underline{\mathbf{s}} = \mathbf{0}$. Thus, due to the minimization objective function, constraints (2.9d) and (2.9e) are binding at optimality, and the admissible interval always corresponds to case (a), where $\underline{\mathbf{s}} = \underline{\mathbf{y}}$ and $\overline{\mathbf{s}} = \overline{\mathbf{y}}$. If, on the other hand, $\mathbf{B} > \mathbf{0}$, two cases are considered:

First, for $\boldsymbol{\alpha} > \mathbf{0}$, it is obvious that $\overline{\mathbf{s}} > \underline{\mathbf{s}}$. Thus, replacing (2.9c) in (2.9b), it is concluded that $\mathbf{Ax}+\mathbf{B}\underline{\mathbf{s}} < \mathbf{g}$ always holds for any value of $\underline{\mathbf{s}} \in [\mathbf{0}, \underline{\mathbf{y}}]$. Due to the minimization objective function in (2.9a), $\underline{\mathbf{s}} = \underline{\mathbf{y}}$ at optimality. Depending on the value of $\boldsymbol{\alpha}$, by substitution, it can be observed from (2.9b) and (2.9c) that:

- If $\mathbf{B}(\overline{\mathbf{y}} - \underline{\mathbf{y}}) \leq \boldsymbol{\alpha}$, then $\mathbf{Ax} + \mathbf{B}\overline{\mathbf{s}} \leq \mathbf{Ax} + \mathbf{B}\overline{\mathbf{y}} \leq \mathbf{g}$ is satisfied for any value of $\overline{\mathbf{s}} \leq \overline{\mathbf{y}}$. Thus, due to the minimization objective function (2.9a), $\overline{\mathbf{s}} = \overline{\mathbf{y}}$ at optimality, which corresponds to case (a).

- Similarly, if $\mathbf{B}(\hat{\mathbf{y}} - \underline{\mathbf{y}}) \leq \boldsymbol{\alpha} < \mathbf{B}(\overline{\mathbf{y}} - \underline{\mathbf{y}})$, then $\hat{\mathbf{y}} \leq \overline{\mathbf{s}} < \overline{\mathbf{y}}$ at optimality, which corresponds to case (b).
- If $\mathbf{0} < \boldsymbol{\alpha} < \mathbf{B}(\hat{\mathbf{y}} - \underline{\mathbf{y}})$, then $\underline{\mathbf{y}} < \overline{\mathbf{s}} < \hat{\mathbf{y}}$ at optimality, which corresponds to case (c).

Second, for $\boldsymbol{\alpha} = \mathbf{0}$, it is concluded that $\underline{\mathbf{s}} = \overline{\mathbf{s}}$. Denote sets $I = [\mathbf{0}, \underline{\mathbf{y}}]$ and $J = (\underline{\mathbf{y}}, \overline{\mathbf{y}}]$, where $I \cap J = \emptyset$ and $I \cup J = [\mathbf{0}, \overline{\mathbf{y}}]$. Assume $\exists\ \underline{\mathbf{s}}, \overline{\mathbf{s}} \in J$, such that $\underline{\mathbf{s}} = \overline{\mathbf{s}}$. This contradicts constraint $\underline{\mathbf{s}} \leq \underline{\mathbf{y}}$ and thus $\underline{\mathbf{s}}, \overline{\mathbf{s}} \notin J$. Therefore, $\underline{\mathbf{s}}, \overline{\mathbf{s}} \in I$ and $\underline{\mathbf{s}} = \overline{\mathbf{s}}$, which corresponds to case (d). □

Consider formulation $[\mathbf{M}']$ where the uncertainty set $\mathcal{U} = [\underline{\mathbf{y}}, \overline{\mathbf{y}}]$ of problem $[\mathbf{M}]$ is substituted with the admissible uncertainty set $[\underline{\mathbf{s}}, \overline{\mathbf{s}}]$ denoted by $\mathcal{U}^A$:

$$[\mathbf{M}']: \quad \min_{\mathbf{x},\mathbf{y}} \quad c_1(\mathbf{x}) + c_2(\mathbf{y}), \tag{2.10a}$$

$$\text{s.t.} \quad \mathbf{A}\mathbf{x} + \mathbf{B}\mathbf{y} \leq \mathbf{g}, \tag{2.10b}$$

$$\mathbf{y} \leq \tilde{\mathbf{s}}, \qquad \forall \tilde{\mathbf{s}} \in \mathcal{U}^A = [\underline{\mathbf{s}}, \overline{\mathbf{s}}] \tag{2.10c}$$

$$\mathbf{x}, \mathbf{y} \geq \mathbf{0}. \tag{2.10d}$$

The following proposition shows the equivalency of problems $[\mathbf{M}]$ and $[\mathbf{M}']$.

Proposition 3. *Problems* $[\mathbf{M}]$ *and* $[\mathbf{M}']$ *have the exact same feasible region.*

Proof. Let $\mathbf{X}$ and $\mathbf{X}'$ be the feasible sets of $[\mathbf{M}]$ and $[\mathbf{M}']$, respectively. To conclude that the two feasible sets are equal, it is sufficient to show that any feasible solution in $\mathbf{X}$ is also feasible for $\mathbf{X}'$ and vice-versa.

First, let $\mathbf{x}', \mathbf{y}' \in \mathbf{X}'$, where $\mathbf{y}' \leq \tilde{\mathbf{s}} \in [\underline{\mathbf{s}}, \overline{\mathbf{s}}]$. Since $[\underline{\mathbf{s}}, \overline{\mathbf{s}}]$ falls into one of the cases of Proposition 2, it satisfies the conditions of Proposition 1. Thus, $\mathbf{x}', \mathbf{y}' \in \mathbf{X}$ as well.

Similarly, let $\mathbf{x}, \mathbf{y} \in \mathbf{X}$, where $\mathbf{y} \leq \tilde{\mathbf{y}} \in [\underline{\mathbf{y}}, \overline{\mathbf{y}}]$. From the constraints of (2.4), it is observed that for values of $\mathbf{z}$ corresponding to $\tilde{\mathbf{y}} \in (\overline{\mathbf{s}}, \overline{\mathbf{y}}]$ constraint (2.4b) becomes redundant. Thus, $\mathbf{y} \leq \overline{\mathbf{s}}$ and it demonstrates that $\mathbf{x}, \mathbf{y} \in \mathbf{X}'$ as well. □

From Proposition 3, it can be concluded that instead of incorporating a budget of uncertainty in problem [$\mathbf{M}$] with partially-ineffective uncertainty set, problem [$\mathbf{M}'$] can be used without changing the feasible region.

The admissible uncertainty set of problem [$\mathbf{M}'$] can be formulated as follows.

$$\mathcal{U}^A := \Big\{ \tilde{\mathbf{s}} \in \mathcal{R}^m : \quad \tilde{\mathbf{s}} = \hat{\mathbf{s}} + \mathbf{z}^+ \odot (\overline{\mathbf{s}} - \hat{\mathbf{s}}) + \mathbf{z}^- \odot (\underline{\mathbf{s}} - \hat{\mathbf{s}}), \quad \mathbf{0} \leq \mathbf{z}^+, \mathbf{z}^- \leq \mathbf{1} \Big\}, \tag{2.11}$$

where $\hat{\mathbf{s}}$ is the middle point of the interval $[\underline{\mathbf{s}}, \overline{\mathbf{s}}]$, and $\mathbf{z}^+$ and $\mathbf{z}^-$ denote positive and negative scaled deviations from $\hat{\mathbf{s}}$.

2.2.2 Effective Interval

The following proposition identifies a subset of the admissible uncertainty set in which the worst-case scenario of the admissible uncertainty set would always occur.

Proposition 4. *The worst-case realization of the admissible uncertainty set $\mathcal{U}^A$ always occurs within interval $[\hat{\mathbf{s}}, \overline{\mathbf{s}}]$, where $\hat{\mathbf{s}}$ is the middle point of the interval $[\underline{\mathbf{s}}, \overline{\mathbf{s}}]$.*

Proof. Using the definition of $\mathcal{U}^A$, it is observed that $[\underline{\mathbf{s}}, \overline{\mathbf{s}}] = [\underline{\mathbf{s}}, \hat{\mathbf{s}}] \cup [\hat{\mathbf{s}}, \overline{\mathbf{s}}]$. Thus, the worst-case of constraint (2.7) can be re-written by considering $\boldsymbol{\beta}(\mathbf{z}^+, \mathbf{z}^-)$ instead of $\boldsymbol{\beta}(\mathbf{r})$, where:

$$\boldsymbol{\beta}(\mathbf{z}^+, \mathbf{z}^-) = \max_{\mathbf{z}^+, \mathbf{z}^-} \quad \mathbf{B}\Big(\hat{\mathbf{s}} + \mathbf{z}^+ \odot (\overline{\mathbf{s}} - \hat{\mathbf{s}}) + \mathbf{z}^- \odot (\underline{\mathbf{s}} - \hat{\mathbf{s}})\Big), \tag{2.12a}$$

$$\text{s.t.} \quad \mathbf{0} \leq \mathbf{z}^+ \leq \mathbf{1}, \tag{2.12b}$$

$$\mathbf{0} \leq \mathbf{z}^- \leq \mathbf{1}. \tag{2.12c}$$

Separating the constant $\mathbf{B}\hat{\mathbf{s}}$ from the objective function and considering dual vectors $\boldsymbol{\eta}$ and $\boldsymbol{\zeta}$ for constraints (2.12b) and (2.12c), respectively, the dual formulation of problem (2.12) is as follows

$$\mathbf{B}\hat{\mathbf{s}} + \min_{\boldsymbol{\eta}, \boldsymbol{\zeta}} \quad \boldsymbol{\eta} + \boldsymbol{\zeta}, \tag{2.13a}$$

$$\text{s.t.} \quad \boldsymbol{\eta} \geq \mathbf{B}(\overline{\mathbf{s}} - \hat{\mathbf{s}}), \tag{2.13b}$$

$$\boldsymbol{\zeta} \geq \mathbf{B}(\underline{\mathbf{s}} - \hat{\mathbf{s}}), \tag{2.13c}$$

$$\boldsymbol{\eta}, \boldsymbol{\zeta} \geq \mathbf{0}. \tag{2.13d}$$

Since $\underline{\mathbf{s}} - \hat{\mathbf{s}} \leq \mathbf{0}$ and $\mathbf{B} \geq \mathbf{0}$ by assumption, constraint (2.13c) is redundant and thus $\boldsymbol{\zeta} = \mathbf{0}$. By removing the redundant constraint (2.13c) and taking the dual of model (2.13) with vector $\mathbf{r}$ as the dual vector corresponding to constraint (2.13b), the following formulation is obtained:

$$\mathbf{B}\hat{\mathbf{s}} + \max_{\mathbf{r}} \quad \mathbf{B}\Big(\mathbf{r} \odot (\overline{\mathbf{s}} - \hat{\mathbf{s}})\Big), \tag{2.14a}$$

$$\text{s.t.} \quad \mathbf{0} \leq \mathbf{r} \leq \mathbf{1}, \tag{2.14b}$$

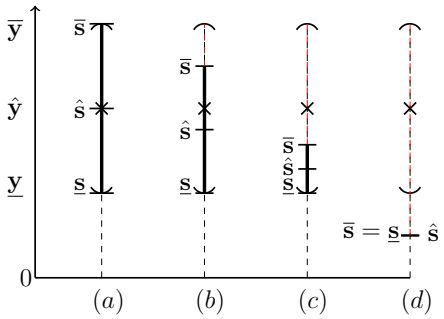

Figure 2.2: Relationships between the original uncertainty set $\mathcal{U} = [\underline{\mathbf{y}}, \overline{\mathbf{y}}]$, the admissible uncertainty set $\mathcal{U}^A = [\underline{\mathbf{s}}, \overline{\mathbf{s}}]$, and the effective uncertainty set $\mathcal{U}^E = [\hat{\mathbf{s}}, \overline{\mathbf{s}}]$ for all possible cases. The horizontal axis shows the four different cases that could occur, and the vertical axis shows the corresponding uncertainty sets and admissible intervals.

which shows $\tilde{\mathbf{s}} \in [\hat{\mathbf{s}}, \overline{\mathbf{s}}]$. □

Proposition 4 shows the equivalency of the uncertainty sets $[\underline{\mathbf{s}}, \overline{\mathbf{s}}]$ and $[\hat{\mathbf{s}}, \overline{\mathbf{s}}]$ in terms of their worst-case scenarios. Throughout this thesis, effective uncertainty set $[\hat{\mathbf{s}}, \overline{\mathbf{s}}]$ is denoted by $\mathcal{U}^E$ where:

$$\mathcal{U}^E := \left\{ \tilde{\mathbf{s}} \in \mathcal{R}^m : \quad \tilde{\mathbf{s}} = \hat{\mathbf{s}} + \mathbf{r} \odot (\overline{\mathbf{s}} - \hat{\mathbf{s}}), \quad \mathbf{0} \leq \mathbf{r} \leq \mathbf{1}. \right\} \tag{2.15}$$

Therefore, the effective uncertainty set $\mathcal{U}^E = [\hat{\mathbf{s}}, \overline{\mathbf{s}}]$ can be used in formulation $[\mathbf{M}']$. In the following section, an effective budget of uncertainty is identified and incorporated in the effective uncertainty set.

2.3 Effective Budget of Uncertainty

This section draws a one-to-one correspondence between the conventional and proposed budget approaches to specify how Γ would impact the solutions of four cases in Proposition

2. Then, an effective budget of uncertainty is identified by mapping the partially-ineffective budgets to effective budgets.

In the conventional budget approach, the worst-case scenario occurs within uncertainty set $[\hat{\mathbf{y}}, \overline{\mathbf{y}}]$ (see Proposition 4), and Γ captures deviations from the nominal value $\hat{\mathbf{y}}$. However, $\hat{\mathbf{s}}$ is the nominal value of the effective uncertainty set $\mathcal{U}^E = [\hat{\mathbf{s}}, \overline{\mathbf{s}}]$, which is not necessarily equal to $\hat{\mathbf{y}}$ as shown in Fig (2.2). In particular, the conventional approach with zero deviation ($\Gamma = 0$) corresponds to solution $\mathbf{y} = \overline{\mathbf{s}}$ in cases (c) and (d) since $\overline{\mathbf{s}} < \tilde{\mathbf{y}} \in [\hat{\mathbf{y}}, \overline{\mathbf{y}}]$. To generate the same solution in $\mathcal{U}^E$, a positive deviation $\mathbf{r}$ from $\hat{\mathbf{s}}$ is required where $\mathbf{y} \leq \hat{\mathbf{s}} + \mathbf{r} \odot (\overline{\mathbf{s}} - \hat{\mathbf{s}})$. Otherwise, for a zero value of $\mathbf{r}$, $\mathcal{U}^E$ would result in $\mathbf{y} = \hat{\mathbf{s}}$, which is different than the solution of the conventional approach with no uncertainty. Thus, to keep the properties of the conventional approach in the proposed approach, such deviations should be allowed but should not be taken into account in the budget of uncertainty constraint for cases (c) and (d).

Similarly, in case (b), when $\tilde{\mathbf{s}} < \hat{\mathbf{y}}$, for any value of Γ, the conventional approach corresponds to $\mathbf{y} = \hat{\mathbf{y}}$. Fig. 2.3 elaborates on case (b) and compares the uncertain parameters in $\mathcal{U}^E$ and $\mathcal{U}^B$ based on their scaled deviations. Recall from Section 2.1 that the conventional budget is ineffective for $\tilde{\mathbf{y}} \in (\overline{\mathbf{s}}, \overline{\mathbf{y}}]$. Intuitively, only the scaled deviations in $\mathcal{U}^B$ corresponding to segment $A'C$ are effective in the conventional approach. It can be proved that normalizing the scaled deviations based on the length of each uncertainty set, segment $A'C$ with uncertainty set $[\underline{\mathbf{y}}, \overline{\mathbf{y}}]$ corresponds to $A'B'$ with uncertainty set $[\underline{\mathbf{s}}, \overline{\mathbf{s}}]$. For segment $A'B'$, solutions are effectively adjusted by an effective budget of uncertainty. Thus, to keep the consistency of the proposed approach with the conventional budget approach, the uncertainty set of the proposed approach is to be able to construct all point

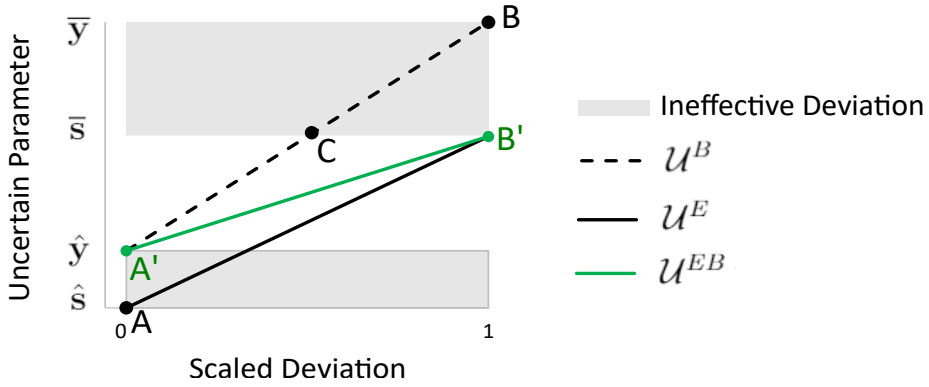

Figure 2.3: Comparison of the uncertain parameters in $\mathcal{U}^B$, $\mathcal{U}^E$, and $\mathcal{U}^{EB}$ for 1 unit of scaled deviation in case (b)

of segment $A'B'$. To do so, AB' corresponding to $\mathcal{U}^E$ is to be mapped to segment $A'B'$. Thus, a shift from $\hat{\mathbf{s}}$ (point A) to $\hat{\mathbf{y}}$ (point A') is required but the required budget for this shift should not be taken into account in the budget of uncertainty constraint. Otherwise, the budget is not effectively used. The shaded regions in Fig. 2.3 show the areas within which the budget of uncertainty of the conventional approach does not impact the solutions. Definition 1 corresponds to an effective uncertainty $\mathcal{U}^{EB}$ where an effective budget Γ^E is incorporated in $\mathcal{U}^E$. Proposition 5 explains a linear mapping between Γ and Γ^E.

Definition 1. *The effective uncertainty set $\mathcal{U}^{EB}$ with an effective budget of uncertainty Γ^E is defined as*

$$\mathcal{U}^{EB} := \Big\{ \tilde{\mathbf{s}} \in \mathcal{R}^m : \quad \tilde{\mathbf{s}} = \hat{\mathbf{s}} + \mathbf{r} \odot (\bar{\mathbf{s}} - \hat{\mathbf{s}}), \tag{2.16a}$$

$$\sum_{i=1}^{m} e_i r_i \leq \Gamma^E, \tag{2.16b}$$

$$\mathbf{v} \leq \mathbf{r} \leq \mathbf{1}. \quad \Big\} \tag{2.16c}$$

where vectors $\mathbf{v}$, $\mathbf{e}$ *are pre-calculated and parameter* Γ^E *is a function of* Γ *as follows:*

$$\mathbf{h} = \frac{1}{2}\Big(1 - \text{sgn}(\hat{\mathbf{y}} - \overline{\mathbf{s}})\Big), \tag{2.17a}$$

$$\mathbf{e} = \mathbf{h} \odot (\frac{\overline{\mathbf{s}} - \hat{\mathbf{s}}}{\overline{\mathbf{y}} - \hat{\mathbf{y}}}), \tag{2.17b}$$

$$\mathbf{v} = \mathbf{h} \odot (\frac{\hat{\mathbf{y}} - \hat{\mathbf{s}}}{\overline{\mathbf{s}} - \hat{\mathbf{s}}}), \tag{2.17c}$$

$$\Gamma^E = \Gamma + \sum_{i=1}^{m} v_i (\frac{\overline{s}_i - \hat{s}_i}{\overline{y}_i - \hat{y}_i}). \tag{2.17d}$$

Proposition 5. *The partially-ineffective budget* Γ *in the uncertainty set* $\mathcal{U}^B$ *is linearly mapped into an effective budget of* Γ^E *in the uncertainty set* $\mathcal{U}^{EB}$.

Proof. Consider $\mathbf{h} = \frac{1}{2}\big(1 - \text{sgn}(\hat{\mathbf{y}} - \overline{\mathbf{s}})\big)$. Based on the definition of $\mathbf{h}$, it is observed that $\mathbf{h} = \mathbf{1}$ for cases (a) and (b), and $\mathbf{h} = \mathbf{0}$ for cases (c) and (d). Since $\mathbf{e}$ is a function of $\mathbf{h}$, constraint (2.16b) ensures Γ^E is effectively used by not taking into account the deviations of case (c) and case (d). Similarly, consider $\mathbf{v} = \mathbf{h} \odot (\frac{\hat{\mathbf{y}} - \hat{\mathbf{s}}}{\overline{\mathbf{s}} - \hat{\mathbf{s}}})$, which takes a value of $\mathbf{0}$ for all cases except case (b), due to $\mathbf{h} = \mathbf{0}$ in cases (c) and (d), and $\hat{\mathbf{y}} = \hat{\mathbf{s}}$ in case (a). The nonzero value of $\mathbf{v}$ is the scaled deviation required to map $\hat{\mathbf{s}}$ to $\hat{\mathbf{y}}$. Thus, $\mathbf{v} \leq \mathbf{r}$ ensures $\hat{\mathbf{s}}$ is mapped to $\hat{\mathbf{y}}$. To ensure the proposed approach allows this mapping without using the budget of uncertainty, Γ is linearly mapped to $\Gamma + \mathbf{v}$, where

$$\sum_{i=1}^{m} h_i r_i \leq \Gamma + \mathbf{v} \tag{2.18}$$

Note that $\mathbf{v}$ and $\mathbf{r}$ are scaled deviations based on the length of $(\overline{\mathbf{s}} - \hat{\mathbf{s}})$, while Γ is an scaled parameter based on the magnitude of $(\overline{\mathbf{y}} - \hat{\mathbf{y}})$. To normalize the scaled deviations, factor

$\frac{\overline{\mathbf{s}}-\hat{\mathbf{s}}}{\overline{\mathbf{y}}-\hat{\mathbf{y}}}$ is multiplied by $\mathbf{v}$ and $\mathbf{r}$. Doing so, formulations (2.16) and (2.17) can be recovered. □

In proposition 5, it was shown that the initial budget of uncertainty can be mapped to an effective budget of uncertainty. The original Γ in the conventional budget approach takes a value within $[0, |m|]$ (Bertsimas and Sim, 2004). Similarly, $\Gamma^E = \Gamma + \sum_{i=1}^{m} v_i \in \left[\sum_{i=1}^{m} v_i, \sum_{i=1}^{m} v_i + |m|\right]$. Term $\sum_{i=1}^{m} v_i$ is constant and is positive only if the uncertain parameter corresponds to the effective interval of case (b). In such a case, $\sum_{i=1}^{m} v_i$ is used for the mapping and only Γ is adjustable in the definition of Γ^E. Particularly, $\Gamma = 0$ in the conventional approach corresponds to $\Gamma^E = \sum_{i=1}^{m} v_i$ in the proposed approach to generate the same solution (point A' of Fig. 2.3). Furthermore, where all uncertain parameters can be entirely utilized, i.e., case (a), for each i, it is concluded: $e_i = 1$, $v_i = 0$, $\hat{s}_i = \hat{y}_i$, $\overline{s}_i = \overline{y}_i$. Therefore $\Gamma^E = \Gamma$ and the proposed approach becomes the same as the previous budget approach. Thus, the proposed column-wise approach for the budget of uncertainty is consistent with the conventional budget approach.

2.4 The Proposed Two-Stage RO Model

This section summarizes a new two-stage robust model to solve RHS uncertainty with effective budget of uncertainty. Given the original uncertainty set $\mathcal{U} = [\underline{\mathbf{y}}, \overline{\mathbf{y}}]$, the first stage solves an auxiliary problem to identify the largest admissible interval $\mathcal{U}^A = [\underline{\mathbf{s}}, \overline{\mathbf{s}}]$, and then the effective uncertainty set $\mathcal{U}^E = [\hat{\mathbf{s}}, \overline{\mathbf{s}}]$ is derived. The second stage problem incorporates the effective budget Γ^E in the effective uncertainty set $\mathcal{U}^E = [\hat{\mathbf{s}}, \overline{\mathbf{s}}]$.

2.4.1 Stage I

The following optimization problem finds the admissible uncertainty set $\mathcal{U}^A = [\underline{\mathbf{s}}, \overline{\mathbf{s}}]$ that has the smallest distance from the original uncertainty set $\mathcal{U} = [\underline{\mathbf{y}}, \overline{\mathbf{y}}]$ (recall Remark 1).

$$\min_{\underline{\mathbf{s}}, \overline{\mathbf{s}}, \boldsymbol{\alpha}, \mathbf{x}} \quad (\overline{\mathbf{y}} - \overline{\mathbf{s}}) + (\underline{\mathbf{y}} - \underline{\mathbf{s}}), \tag{2.19a}$$

$$\text{s.t.} \quad \mathbf{A}\mathbf{x} + \mathbf{B}\underline{\mathbf{s}} + \boldsymbol{\alpha} \leq \mathbf{g}, \tag{2.19b}$$

$$\boldsymbol{\alpha} \geq \mathbf{B}(\overline{\mathbf{s}} - \underline{\mathbf{s}}), \tag{2.19c}$$

$$\overline{\mathbf{s}} \leq \overline{\mathbf{y}}, \tag{2.19d}$$

$$\underline{\mathbf{s}} \leq \underline{\mathbf{y}}, \tag{2.19e}$$

$$\mathbf{x}, \underline{\mathbf{s}}, \overline{\mathbf{s}}, \boldsymbol{\alpha} \geq \mathbf{0}. \tag{2.19f}$$

After solving this optimization problem, the effective uncertainty set $\mathcal{U}^E$ is calculated and is used as the input of stage II.

2.4.2 Stage II

Given the effective uncertainty set obtained in stage I, parameter Γ^E and vectors $\mathbf{v}$ and $\mathbf{e}$ are pre-calculated via (2.17). Then, the following optimization problem that incorporates

the effective budget of uncertainty in the robust model is solved.

$$\min_{\mathbf{x},\mathbf{y},\mathbf{r}} \quad c_1(\mathbf{x}) + c_2(\mathbf{y}), \tag{2.20a}$$

$$\text{s.t} \quad \mathbf{A}\mathbf{x} + \mathbf{B}\mathbf{y} \leq \boldsymbol{g}, \tag{2.20b}$$

$$\mathbf{y} \leq \tilde{\mathbf{s}} \tag{2.20c}$$

$$\tilde{\mathbf{s}} = \hat{\mathbf{s}} + \mathbf{r} \odot (\overline{\mathbf{s}} - \hat{\mathbf{s}}), \tag{2.20d}$$

$$\sum_{i=1}^{m} e_i r_i \leq \Gamma^E, \tag{2.20e}$$

$$\mathbf{v} \leq \mathbf{r} \leq \mathbf{1}, \tag{2.20f}$$

$$\mathbf{x}, \mathbf{y} \geq \mathbf{0}. \tag{2.20g}$$

The proposed two-stage approach provides insights on the admissibility of resources with uncertain parameters in the RHS of constraints. From a managerial point of view, the trade-off between the robustness and objective function value can be explicitly observed since changing the uncertainty budget would change the objective function. This would allow for a more intuitive way for decision makers to determine the level of conservatism of the robust solutions and decide on the value of the budget of uncertainty in the model.

Chapter 3

Robust SCED of Mixed AC-HVDC Multi-Area Power Systems

This chapter addresses the wind power uncertainty of the security-constrained economic dispatch (SCED) problem in a mixed alternating current-high voltage direct current (AC-HVDC) power system. The chapter is organized as follows: Section 3.1 provides the power flow equations in a conventional AC system. Section 3.2 describes the main components of a mixed AC-HVDC power system and formulates the SCED problem in a mixed AC-HVDC power system. In Section 3.5, the proposed robust approach of Chapter 2 is applied to the SCED problem in mixed AC-HVDC multi-area power systems.

3.1 Power Flow Eqution in AC Power Systems

Any power system constitutes of three major parts: (i) generating units, (ii) transmission systems, and (iii) loads (Kundur et al., 1994). A power system is represented by a network of buses and transmission lines as shown in Fig. 3.1.

DC power flow is a simplified version of a full power flow, where the voltage magnitude at all buses is assumed to be 1 per-unit (pu) and the resistance of all transmission lines are neglected (Vrakopoulou et al., 2013). Considering a power system with N buses and L transmission lines, let P_i denote the power injection at bus i. Thus, DC power flow equations can be written as:

$$P_i = \sum_{\substack{j=1 \\ j \neq i}}^{N} B_{ij}(\theta_i - \theta_j), \quad \forall i \in N \tag{3.1}$$

where B_{ij} is the admittance of line connecting buses i and j, and θ_i represents the voltage angle of bus i (Vrakopoulou et al., 2013). Let F_{ij} denote the DC power flow of the

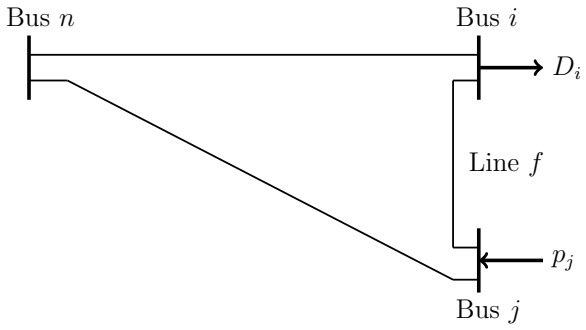

Figure 3.1: A three-bus power system with load D_i and generation p_j.

transmission line connecting buses i and j. Thus:

$$F_{ij} = B_{ij}(\theta_i - \theta_j). \quad \forall i, j \in N \tag{3.2}$$

DC load flow equations (3.1) and (3.2) can be written in matrix form as follows:

$$\mathbf{P} = \mathbf{B}\boldsymbol{\theta}, \tag{3.3}$$

$$\mathbf{F} = \mathbf{M}\boldsymbol{\theta}, \tag{3.4}$$

where matrix $\mathbf{M}$ is directly determined from line data and network characteristics (Chang et al., 1993). For a given line f connecting buses i to j, M_{ft} is defined as follows (Van den Bergh and Delarue, 2015):

$$M_{ft} = \begin{cases} B_{ij} & \text{for t=i} \\ -B_{ij} & \text{for t=j} \\ 0 & \text{for } t \neq i \text{ and } t \neq j \ . \end{cases} \tag{3.5}$$

In equations (3.3) and (3.5), the matrices $\mathbf{B}$ and $\mathbf{M}$ are singular and cannot be inverted. Selecting an arbitrary bus as a reference bus and eliminating the elements associated with the reference bus, sub-matrices $\mathbf{B'}$ and $\mathbf{M'}$, and sub-vectors $\mathbf{P'}$, $\boldsymbol{\theta'}$, and $\mathbf{F'}$ can be obtained. Therefore, equations (3.3) and (3.5) can be re-written as follows:

$$\mathbf{P'} = \mathbf{B'}\boldsymbol{\theta'} \rightarrow \boldsymbol{\theta'} = \mathbf{B'}^{-1}\mathbf{P'}, \tag{3.6}$$

$$\mathbf{F}' = \mathbf{M}'\boldsymbol{\theta}'. \tag{3.7}$$

Substituting $\boldsymbol{\theta}'$ from equation (3.6) to equation (3.7), the following equation is obtained:

$$\mathbf{F}' = \mathbf{M}'\mathbf{B}'^{-1}\mathbf{P}', \tag{3.8}$$

where in matrix $\mathbf{G^I} = \mathbf{M}'\mathbf{B}'^{-1}$, the rows and columns correspond to the transmission lines and buses, respectively. This matrix is called the generation shift distribution factor and denotes the sensitivity of power flow of a given internal line f to power injection at a given internal bus i Van den Bergh and Delarue (2015). Thus, DC line flow equations can be written as follows with respect to injections at buses (Li et al., 2016a):

$$F_f = \sum_{i=1}^{N} G^I_{f,i}(p_i - D_i), \quad \forall f \in L. \tag{3.9}$$

3.2 Mixed AC-HVDC Multi-Area Power Systems

The development of mixed AC-HVDC systems has resulted in significant enhancements in the controllability of the transferred power, system efficiency, and operational flexibility (Kundur et al., 1994). A mixed AC-HVDC power system has three main components: AC system, converters, and HVDC tie-lines, Fig. 3.2a.

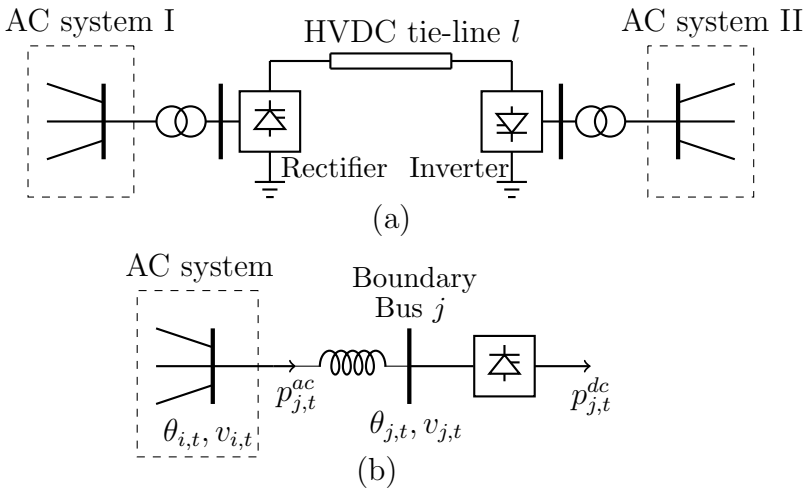

Figure 3.2: (a) Model of a mixed AC-HVDC multi-area power system. (b) Reduced converter model with external injections instead of tie-line flows.

3.2.1 AC Power Systems

In this section, the power flow equations associated with the AC system for the SCED problem are presented. These equations consist of the operational limits and power balance requirements of the AC system.

$$\sum_{i\in\mathcal{N}_a^I}\left(\sum_{g\in\mathcal{G}_i} p_{g,t} + \sum_{k\in\mathcal{K}_i} p^W_{k,t} - D_{i,t}\right) = \sum_{j\in\mathcal{N}_a^C} p^{ac}_{j,t}, \qquad \forall a\in\mathcal{A}, t\in\mathcal{T} \quad (3.10)$$

$$\underline{F}_f \le \sum_{i\in\mathcal{N}_a^I} G^I_{f,i}\left(\sum_{g\in\mathcal{G}_i} p_{g,t} + \sum_{k\in\mathcal{K}_i} p^W_{k,t} - D_{i,t}\right) \le \overline{F}_f, \qquad \forall a\in\mathcal{A}, f\in\mathcal{F}_a, \forall t\in\mathcal{T} \quad (3.11)$$

$$-U^d_g.\Delta t \le p_{g,t} - p_{g,t-1} \le U^u_g.\Delta t, \qquad \forall g\in\mathcal{G}_i, i\in\mathcal{N}_a^I, a\in\mathcal{A}, t\in\mathcal{T} \quad (3.12)$$

$$\sum_{i\in\mathcal{N}_a^I}\sum_{g\in\mathcal{G}_i} r^+_{g,t} \ge R^u_{a,t}, \qquad \forall a\in\mathcal{A}, t\in\mathcal{T} \quad (3.13)$$

$$\sum_{i \in \mathcal{N}_a^I} \sum_{g \in \mathcal{G}_i} r_{g,t}^{-} \geq R_{a,t}^{d}, \qquad \forall a \in \mathcal{A}, t \in \mathcal{T} \quad (3.14)$$

$$r_{g,t}^{+} \leq \min \left\{ \overline{P}_g - p_{g,t} \, , \, U_g.\Delta t \right\}, \qquad \forall g \in \mathcal{G}_i, i \in \mathcal{N}_a^I, a \in \mathcal{A}, t \in \mathcal{T} \quad (3.15)$$

$$r_{g,t}^{-} \leq \min \left\{ p_{g,t} - \underline{P}_g \, , \, D_g.\Delta t \right\}, \qquad \forall g \in \mathcal{G}_i, i \in \mathcal{N}_a^I, a \in \mathcal{A}, t \in \mathcal{T} \quad (3.16)$$

$$\underline{P}_g \leq p_{g,t} \leq \overline{P}_g, \qquad \forall g \in \mathcal{G}_i, i \in \mathcal{N}_a^I, a \in \mathcal{A}, t \in \mathcal{T} \quad (3.17)$$

$$p_{k,t}^{W} \leq \tilde{W}_{k,t}. \qquad \forall k \in \mathcal{K}_i, i \in \mathcal{N}_a^I, a \in \mathcal{A}, t \in \mathcal{T} \quad (3.18)$$

Equation (3.10) represents the power balance requirement of each area. The transmission capacity of internal lines are taken into account in constraint (3.11). Constraint (3.12) represents the upper and lower limits of the ramping rates of conventional generators. To respond to unforeseen power outages, upward/downward reserve requirements are added in constraints (3.13) and (3.14), respectively. Upward/downward reserves denote a fraction of the generator's capacity that can be available to increase/decrease the unit's power output in a short amount of time (e.g., 10 minutes) (Li et al., 2013). Upward and downward reserve capacity constraints are presented in (3.15) and (3.16). Constraints (3.17) and (3.18) represent the output limits of conventional generators and wind farms, respectively.

3.2.2 Converters and HVDC Tie-Lines

Converters, i.e., rectifiers or inverters, are the intersections of AC grids and HVDC tie-lines as shown in Fig. 3.2(a) (Kundur et al., 1994). Unlike the AC systems where power flow of transmission lines depend on the voltage angles of two ends of transmission lines, in a mixed AC-HVDC system, tie-line flows are controllable variables that can be adjusted based on

the net power difference between generation and load in each area. Therefore, in a mixed AC-HVDC system, the SCED problem can be decomposed into several subproblems such that the SCED problem associated with each area can be solved individually by considering a controllable net power exchange with neighboring areas. In this thesis, converter losses are not considered, and for each area, the relationships between the net AC and DC power injections can be expressed as:

$$\sum_{j \in \mathcal{N}_a^C} p_{j,t}^{ac} = \sum_{j \in \mathcal{N}_a^C} p_{j,t}^{dc}. \qquad \forall a \in \mathcal{A}, \forall t \in \mathcal{T} \tag{3.19}$$

A mixed AC-HVDC multi-area power system is decomposed into $|\mathcal{A}|$ single-area systems by modeling the HVDC tie-line flows as power injections/absorption at the boundary buses. Therefore, each HVDC tie-line is modeled as two external DC power injections with equal magnitudes but in opposite directions. Equation (3.20) describes the relationship between tie-line flows and external DC power injections to each area. In (3.20), matrix $\mathbf{H}$ consists of only 0 and 1 elements. For example, $H_{li} = 1$ indicates an external injection to bus i, which corresponds to the power flow of tie-line l. Furthermore, the operational limits of the HVDC tie-lines are presented in equations (3.21).

$$\mathbf{H}\mathbf{p}^{dc} = \mathbf{0}, \tag{3.20}$$

$$\underline{L}_j \leq p_{j,t}^{dc} \leq \overline{L}_j. \qquad \forall j \in \mathcal{N}_a^C, \forall a \in \mathcal{A}, \forall t \in \mathcal{T} \tag{3.21}$$

3.3 Wind Power Admissible Interval

Considering a prediction error $e_{k,t}$, the available wind power $\tilde{W}_{k,t}$ can vary within the uncertainty set $\tilde{W}_{k,t} \in [\hat{W}_{k,t} - e_{k,t}, \hat{W}_{k,t} + e_{k,t}]$, where $\underline{W}_{k,t} = \hat{W}_{k,t} - e_{k,t}$ and $\overline{W}_{k,t} = \hat{W}_{k,t} + e_{k,t}$. In the SCED problem, the available wind power cannot be fully absorbed in case of violations in the spinning reserve or transmission flow constraints. In such a scenario, wind power curtailment is required. The admissible interval of wind power output $[\underline{s}_{k,t}, \overline{s}_{k,t}]$ is defined as the largest subset of wind power generation which results in feasible solutions to the SCED problem:

$$\underline{s}_{k,t} \leq p^W_{k,t} \leq \overline{s}_{k,t}, \qquad \forall k \in \mathcal{K}_i, \forall i \in \mathcal{N}^I_a, \forall a \in \mathcal{A}, \forall t \in \mathcal{T} \tag{3.22}$$

$$\overline{s}_{k,t} \leq \overline{W}_{k,t}, \qquad \forall k \in \mathcal{K}_i, \forall i \in \mathcal{N}^I_a, \forall a \in \mathcal{A}, \forall t \in \mathcal{T} \tag{3.23}$$

$$\underline{s}_{k,t} \leq \underline{W}_{k,t}, \qquad \forall k \in \mathcal{K}_i, \forall i \in \mathcal{N}^I_a, \forall a \in \mathcal{A}, \forall t \in \mathcal{T} \tag{3.24}$$

where $\overline{s}_{k,t} = 0$ and $\overline{s}_{k,t} = \overline{W}_{k,t}$ respectively refer to full curtailment and no curtailment of wind power that can potentially occur due to security issues. To ensure the system security, the worst-case scenarios of transmission constraint (3.11) and reserve constraints (3.13) and (3.14) should be satisfied. Constraints (3.25) to (3.28) correspond to the worst-case scenarios of constraints (3.11) and (3.13)-(3.14), respectively. Since $p^W_{k,t} \leq \overline{s}_{k,t}$, system security will be guaranteed for any $\overline{s}_{k,t}$ satisfying the following constraints.

$$\max_{\overline{s}_{k,t}} \left\{ \sum_{i \in \mathcal{N}^I_a} G^I_{f,i} \left(\sum_{g \in \mathcal{G}_i} p_{g,t} + \sum_{k \in \mathcal{K}_i} \overline{s}_{k,t} - D_{i,t} \right) \right\} \leq \overline{F}_f, \qquad \forall a \in \mathcal{A}, \forall f \in \mathcal{F}_a, \forall t \in \mathcal{T} \tag{3.25}$$

$$\min_{\overline{s}_{k,t}} \left\{ \sum_{i \in \mathcal{N}^I_a} G^I_{f,i} \left(\sum_{g \in \mathcal{G}_i} p_{g,t} + \sum_{k \in \mathcal{K}_i} \overline{s}_{k,t} - D_{i,t} \right) \right\} \geq \underline{F}_f, \qquad \forall a \in \mathcal{A}, \forall f \in \mathcal{F}_a, \forall t \in \mathcal{T} \tag{3.26}$$

$$\min_{\overline{s}_{k,t}} \left\{ \sum_{i \in \mathcal{N}_a^I} \left(\sum_{g \in \mathcal{G}_i} p_{g,t} + \sum_{g \in \mathcal{G}_i} r_{g,t}^{+} + \sum_{k \in \mathcal{K}_i} \overline{s}_{k,t} - D_{i,t} \right) - \sum_{j \in \mathcal{N}_a^C} p_j^{ac} \right\} \geq R_{a,t}^{u}, \quad \forall a \in \mathcal{A}, \forall t \in \mathcal{T} \quad (3.27)$$

$$\min_{\overline{s}_{k,t}} \left\{ \sum_{i \in \mathcal{N}_a^I} \left(D_{i,t} - \sum_{g \in \mathcal{G}_i} p_{g,t} + \sum_{g \in \mathcal{G}_i} r_{g,t}^{-} - \sum_{k \in \mathcal{K}_i} \overline{s}_{k,t} \right) + \sum_{j \in \mathcal{N}_a^C} p_j^{ac} \right\} \geq R_{a,t}^{d}. \quad \forall a \in \mathcal{A}, \forall t \in \mathcal{T} \quad (3.28)$$

3.4 Effective Budget of Uncertainty

As shown in Section (2.3), for a given $[\hat{s}_{k,t}, \overline{s}_{k,t}]$, the following polyhedral uncertainty set can be used in the SCED problem where an effective budget of uncertainty Γ^E is considered:

$$\mathcal{U}^{EB} := \Big\{ \tilde{s}_{k,t} : \quad \tilde{s}_{k,t} = \hat{s}_{k,t} + r_{k,t}(\overline{s}_{k,t} - \hat{s}_{k,t}), \quad \forall k \in \mathcal{K}_i, \forall i \in \mathcal{N}_a^I, \forall a \in \mathcal{A}, \forall t \in \mathcal{T} \quad (3.29a)$$

$$\sum_{i \in \mathcal{N}_a^I} \sum_{k \in \mathcal{K}_i} e_{k,t}.r_{k,t} \leq \Gamma_{a,t}^{E}, \qquad \forall a \in \mathcal{A}, \forall t \in \mathcal{T} \quad (3.29b)$$

$$v_{k,t} \leq r_{k,t} \leq 1, \qquad \forall a \in \mathcal{A}, \forall t \in \mathcal{T} \Big\} \quad (3.29c)$$

where parameters $e_{k,t}$, $v_{k,t}$, and $\Gamma_{a,t}^{E}$ are calculated based on Section 2.3.

3.5 Robust SCED Formulation

In this section, the proposed two-stage robust approach of Chapter 2 is applied to the SCED problem with right-hand side (RHS) uncertainty, where vectors $\underline{\mathbf{y}}$, $\hat{\mathbf{y}}$, $\tilde{\mathbf{y}}$ and $\overline{\mathbf{y}}$ of the proposed approach respectively correspond to parameters $\underline{W}_{k,t}$, $\hat{W}_{k,t}$, $\tilde{W}_{k,t}$, and $\overline{W}_{k,t}$. Stage I of the proposed optimization approach solves an auxiliary problem to identify the

admissible and effective uncertainty sets. Then, Stage II uses the optimal solution of the first stage and solves the SCED problem with an effective budget of uncertainty.

3.5.1 Stage I

The auxiliary optimization problem (3.30) is used to find the largest admissible wind power interval $[\underline{s}_{k,t}, \overline{s}_{k,t}]$:

$$\min_{\underline{\boldsymbol{s}},\overline{\boldsymbol{s}},\boldsymbol{p},\boldsymbol{\alpha},\boldsymbol{\eta},\boldsymbol{\zeta},\boldsymbol{\beta}} \quad \sum_{t\in\mathcal{T}}\sum_{a\in\mathcal{A}}\sum_{i\in\mathcal{N}_a^I}\sum_{k\in\mathcal{K}_i}\left(\overline{W}_{k,t}-\overline{s}_{k,t}\right)+\left(\underline{W}_{k,t}-\underline{s}_{k,t}\right) \tag{3.30a}$$

$$\text{s.t.} \quad \sum_{i\in\mathcal{N}_a^I} G^I_{f,i}\left(\sum_{g\in\mathcal{G}_i} p_{g,t}-D_{i,t}+\sum_{k\in\mathcal{K}_i}\underline{s}_{k,t}\right)+\sum_{i\in\mathcal{N}_a^I}\sum_{k\in\mathcal{K}_i}\alpha_{k,f,t}\le \overline{F}_f, \tag{3.30b}$$
$$\forall k\in\mathcal{K}_i,\forall i\in\mathcal{N}_a^I,\forall a\in\mathcal{A},\forall f\in\mathcal{F}_a,\forall t\in\mathcal{T}$$

$$\alpha_{k,f,t}\ge G^I_{f,i}(\overline{s}_{k,t}-\underline{s}_{k,t}), \qquad \forall k\in\mathcal{K}_i,\forall i\in\mathcal{N}_a^I,\forall a\in\mathcal{A},\forall f\in\mathcal{F}_a,\forall t\in\mathcal{T} \tag{3.30c}$$

$$\sum_{i\in\mathcal{N}_a^I} G^I_{f,i}\left(\sum_{g\in\mathcal{G}_i} p_{g,t}-D_{i,t}+\sum_{k\in K_i}\underline{s}_{k,t}\right)-\sum_{i\in\mathcal{N}_a^I}\sum_{k\in\mathcal{K}_i}\zeta_{k,f,t}\ge \underline{F}_f, \tag{3.30d}$$
$$\forall k\in\mathcal{K}_i,\forall i\in\mathcal{N}_a^I,\forall a\in\mathcal{A},\forall f\in\mathcal{F}_a,\forall t\in\mathcal{T}$$

$$\zeta_{k,f,t}\ge -G^I_{f,i}(\overline{s}_{k,t}-\underline{s}_{k,t}), \qquad \forall k\in\mathcal{K}_i,\forall i\in\mathcal{N}_a^I,\forall a\in\mathcal{A},\forall f\in\mathcal{F}_a,\forall t\in\mathcal{T} \tag{3.30e}$$

$$\sum_{i\in\mathcal{N}_a^I}\left(\sum_{g\in\mathcal{G}_i} p_{g,t}+\sum_{g\in\mathcal{G}_i} r^+_{g,t}-D_{i,t}+\sum_{k\in\mathcal{K}_i}\underline{s}_{k,t}-\sum_{k\in\mathcal{K}_i}\eta_{k,t}\right)\ge \sum_{j\in\mathcal{N}_a^C} p_j^{ac}+R^u_{a,t}, \tag{3.30f}$$
$$\forall a\in\mathcal{A},\forall t\in\mathcal{T}$$

$$\eta_{k,t}\ge -(\overline{s}_{k,t}-\underline{s}_{k,t}), \qquad \forall k\in\mathcal{K}_i,\forall i\in\mathcal{N}_a^I,\forall a\in\mathcal{A},\forall t\in\mathcal{T} \tag{3.30g}$$

$$\sum_{i\in\mathcal{N}_a^I}\left(\sum_{g\in\mathcal{G}_i}p_{g,t}-\sum_{g\in\mathcal{G}_i}r_{g,t}^{-}-D_{i,t}+\sum_{k\in\mathcal{K}_i}\underline{s}_{k,t}+\sum_{k\in\mathcal{K}_i}\beta_{k,t}\right)\leq\sum_{j\in\mathcal{N}_a^C}p_j^{ac}-R_{a,t}^{d},\qquad\forall a\in\mathcal{A},\forall t\in\mathcal{T}\tag{3.30h}$$

$$\beta_{k,t}\geq\overline{s}_{k,t}-\underline{s}_{k,t},\qquad\forall k\in\mathcal{K}_i,\forall i\in\mathcal{N}_a^I,\forall a\in\mathcal{A},\forall t\in\mathcal{T}\tag{3.30i}$$

$$\overline{s}_{k,t}\leq\overline{W}_{k,t},\qquad\forall k\in\mathcal{K}_i,\forall i\in\mathcal{N}_a^I,\forall a\in\mathcal{A},\forall t\in\mathcal{T}\tag{3.30j}$$

$$\underline{s}_{k,t}\leq\underline{W}_{k,t},\qquad\forall k\in\mathcal{K}_i,\forall i\in\mathcal{N}_a^I,\forall a\in\mathcal{A},\forall t\in\mathcal{T}\tag{3.30k}$$

$$\boldsymbol{\alpha},\boldsymbol{\eta},\boldsymbol{\zeta},\boldsymbol{\beta}\geq\mathbf{0},\tag{3.30l}$$

where dual vectors $\boldsymbol{\alpha},\boldsymbol{\eta},\boldsymbol{\zeta},\boldsymbol{\beta}$ correspond to constraints (3.25) and (3.28). The optimal solution of the auxiliary problem (3.30) corresponds to the largest admissible wind power interval within which the system security is guaranteed. The effective uncertainty set $[\hat{s}_{k,t},\overline{s}_{k,t}]$, within which the worst-case scenario of the admissible wind power interval occurs as shown in Section 2.2, is used in the second stage of the proposed approach.

3.5.2 Stage II

In the second-stage of the problem, objective function (3.31), which minimizes the total operation cost, is considered. In (3.31), the first and the second terms are respectively associated with the generation and wind power curtailment costs under the worst-case

scenario.

$$\min_{p_{g,t},p^W_{k,t}} \left\{ \sum_{t\in\mathcal{T}} \sum_{a\in\mathcal{A}} \sum_{i\in\mathcal{N}^I_a} \sum_{g\in\mathcal{G}_i} C_g p_{g,t} \ + \max_{\tilde{s}_{k,t}} \left[\sum_{t\in\mathcal{T}} \sum_{a\in\mathcal{A}} \sum_{i\in\mathcal{N}^I_a} \sum_{k\in\mathcal{K}_i} \sigma_k \big(\tilde{s}_{k,t} - p^W_{k,t}\big) \right] \right\} \tag{3.31}$$

The inner maximization term corresponds to the worst-case wind curtailment cost and the penalty factor σ_k is set to the maximum generation cost of conventional generators such that the dispatch priority is given to wind power generators rather than conventional generating units Li et al. (2016a).

In the objective function (3.31), $\tilde{s}_{k,t}$ should be identified first, and then the optimal solutions are obtained. Using duality theorems, and considering the definition of the uncertainty set $\mathcal{U}^{EB}$ in (3.29), the corresponding linear reformulation of the objective function is presented in (3.32)-(3.34):

$$\min_{p_{g,t},p^W_{k,t}} \left\{ \sum_{t\in\mathcal{T}} \sum_{a\in\mathcal{A}} \sum_{i\in\mathcal{N}^I_a} \sum_{g\in\mathcal{G}_i} C_g p_{g,t} + \sum_{t\in\mathcal{T}} \sum_{a\in\mathcal{A}} \sum_{i\in\mathcal{N}^I_a} \sum_{k\in\mathcal{K}_i} \sigma_k \big(\hat{s}_{k,t} + \mu_{k,t} - v_{k,t}\lambda_{k,t} + \Gamma^E_{a,t}\xi_{a,t} - p^W_{k,t}\big) \right\} \tag{3.32}$$

$$\mu_{k,t} - \lambda_{k,t} + e_{k,t}\xi_{a,t} \geq (\overline{s}_{k,t} - \hat{s}_{k,t}), \qquad \forall k \in \mathcal{K}_i, \forall i \in \mathcal{N}^I_a, \forall a \in \mathcal{A}, \forall t \in \mathcal{T} \tag{3.33}$$

$$\mu_{k,t}, \lambda_{k,t}, \xi_{a,t} \geq 0, \qquad \forall k \in \mathcal{K}_i, \forall i \in \mathcal{N}^I_a, \forall a \in \mathcal{A}, \forall t \in \mathcal{T} \tag{3.34}$$

where dual variables $\mu_{k,t}$ and $\lambda_{k,t}$ correspond to the upper and lower limits of constraint (3.29c), respectively, and dual variable $\xi_{a,t}$ corresponds to constraint (3.29b).

The second-stage robust SCED problem in a mixed AC-HVDC with the effective

budget of uncertainty is summarized as follows:

$$
\begin{cases}
\text{Objective Function:} & \text{Equation (3.31)}, \\
\text{s.t.} & \text{Equations (3.10)} - \text{(3.17)}, \\
& 0 \leq p^W_{k,t} \leq \tilde{s}_{k,t}, \qquad \forall k \in \mathcal{K}_i, \forall i \in \mathcal{N}^I_a, \forall a \in \mathcal{A}, \forall t \in \mathcal{T} \\
& \text{Equations (3.19)} - \text{(3.21)}, \\
& \text{Equations (3.29)}, \text{(3.33)} - \text{(3.34)}.
\end{cases}
$$

Chapter 4

Numerical Results

In this chapter, the performance of the proposed RO approach for the SCED problem is examined on three systems. In Section 4.1, the data and system settings are explained. In Section 4.2, the proposed RO approach is applied to the SCED in a simple single-area test system for the purpose of demonstration. This section examines the performance of the proposed approach in terms of the effectiveness of the budget of uncertainty in comparison to that of the conventional budget of uncertainty approach. Section 4.3 addresses the challenges of the SCED problem in a two-area mixed AC-HVDC system and demonstrates the merits of the proposed approach in such systems in terms of robustness, reliability, and power transfer controllability between areas of a mixed AC-HVDC system. Sensitivity of the solutions to system parameters is reviewed in this section as well. Finally, Section 4.4 applies the RO approach to a three-area AC-HVDC system with higher wind power penetration that captures the complexity of real-world power systems. Various power transfer strategies are introduced in this section to further evaluate the performance of the

proposed approach in AC and mixed AC-HVDC systems.

The analyses carried out throughout this chapter fall into one of the followings: day-ahead, look-ahead, or real-time. Day-ahead optimization considers the predicted data of the available wind power for the next 24 hours and solves the SCED problem for a 24-hour time horizon with 1-hour intervals. Look-ahead optimization is based on a more up-to-date wind power prediction and considers the wind power for the next 6 hours with 15-minutes intervals (Lorca and Sun, 2017). Intra-day optimization considers the actual realization of the wind power in real-time to solve the SCED problem.

All results reported in this chapter are obtained using the C++ and CPLEX 12.7.1 combination.

4.1 Test Systems

In this Section, the single-area, two-area, and three-area test systems are introduced. In all test systems, each area is represented by the IEEE reliability test system (RTS) (Grigg et al., 1999).

In the single-area system, a 24-hour time horizon is considered and the SCED problem is executed every hour (day-ahead optimization). Fig. 4.1(a) represents the hourly load of the single-area test system. In the single-area test system, two instances are considered. The first-instance is a small-scale system including two wind farms with wind power profile #1 (Fig. 4.2(a)) added to buses 113 and 116 of the IEEE RTS. The second instance emphasizes on higher wind power penetration (Lopez et al., 2012) and therefore,

two additional wind farms with wind power profile #2, shown in Fig. 4.2(b), are added to buses 118 and 108.

In the two-area test system, a 6-hour time horizon is considered and the SCED problem is executed every 15 minutes (look-ahead optimization). The two-area test system consists of two tie-lines and is obtained by removing area 3 and tie-lines 3,4, and 5 from Fig. 4.3. Fig. 4.1.(b) represents the hourly load of this test system. In this test system, two wind farms with wind profiles #3 and #4, shown in Fig. 4.2(c) and Fig. 4.2(d), are added to buses 113 of area 1 and 208 of area 2, respectively.

In the three-area system, a 6-hour time horizon is used and the SCED problem is executed every 15 minutes (look-ahead optimization). The three-area system is shown in Fig. 4.3. In this test system, three wind farms with wind profile #3, Fig. 4.2(c), are added to buses 113 and 117 of area 1 as well as bus 301 of area 3. Also, two wind farms with wind profile #4, Fig. 4.2(d), are connected to buses 119 of area 1 and 309 of area 3. There are no wind power plant in area 2. The total capacity of wind power generation in

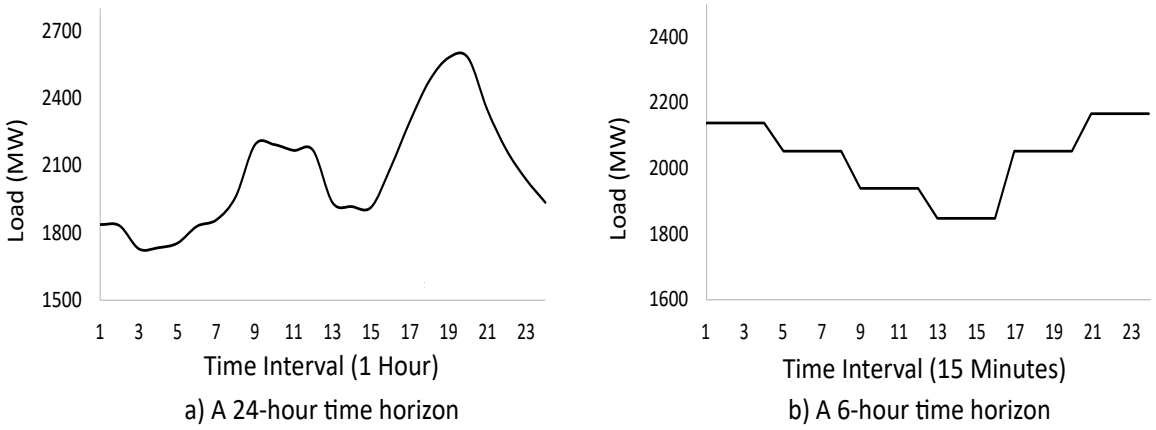

Figure 4.1: Hourly load profiles

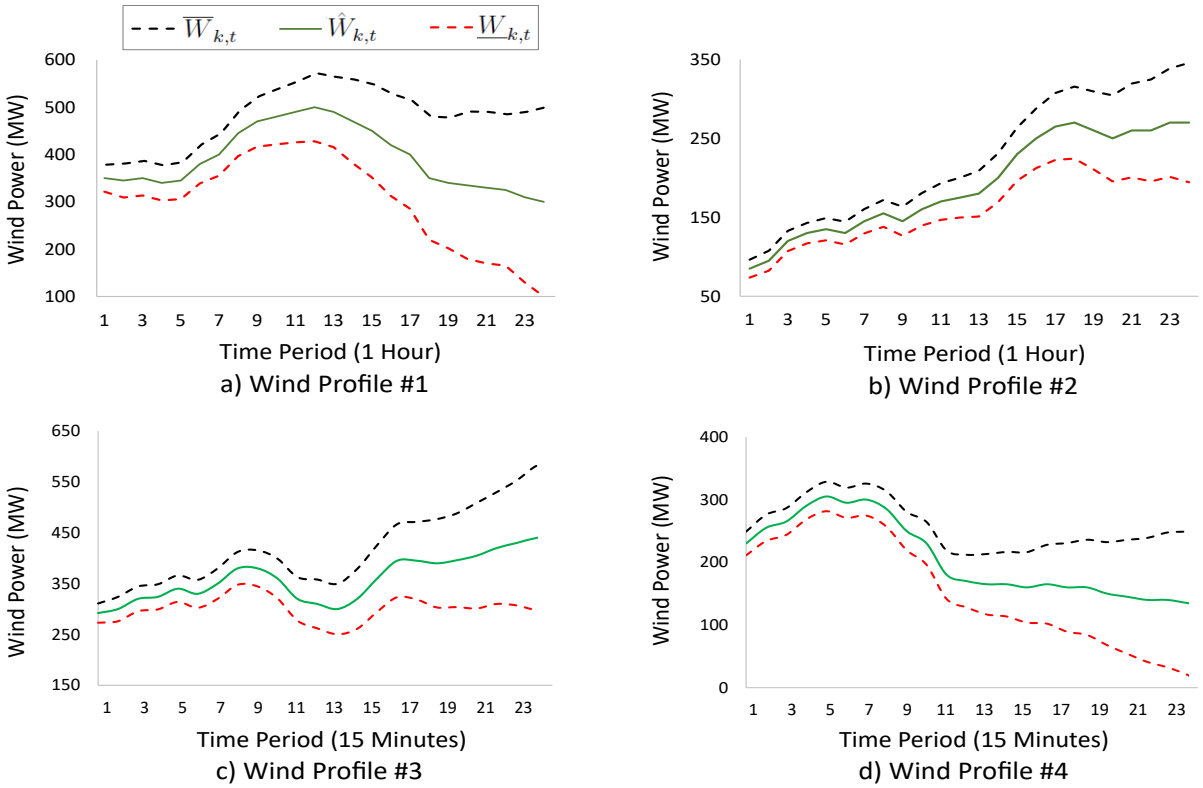

Figure 4.2: Nominal value, upper bound, and lower bound of the predicted wind power

the three-area test system is 2500 MW which is approximately 23% of the total capacity of conventional generators. To accommodate for the increased power generation capacity, the hourly load of Fig. 4.1(b) is increased by 10%, 50%, and 10% in areas 1 to 3, respectively.

In all test systems, the upward spinning reserve requirement $R^u_{a,t}$ is set to 400MW, which is equal to the maximum capacity of conventional generators (Li et al., 2016a), and the downward spinning reserve requirement $R^d_{a,t}$ is 300MW. These settings are compatible with the power system stability requirements described by Kundur et al. (2004).

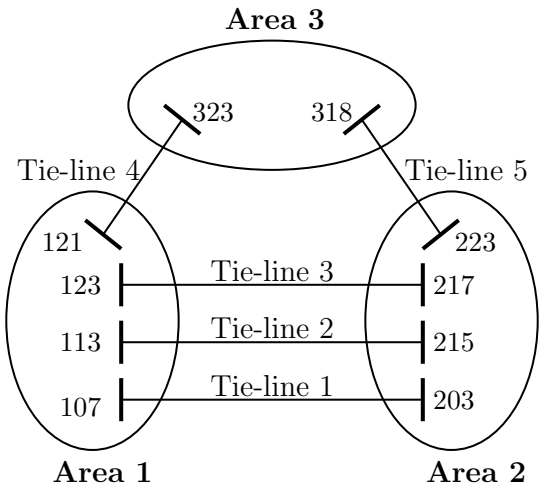

Figure 4.3: Abstract schematic of the multi-area power system

4.2 Single-Area Test System

This test system is designed to demonstrate the performance of the proposed approach in the day-ahead SCED optimization problem and to compare the effectiveness of the proposed approach against the conventional approach for various budgets of uncertainty. Section 4.2.1 illustrates the admissible wind power interval in the first instance of the single-area test system and demonstrates the effectiveness of the proposed approach. Section 4.2.2 highlights the merits of the proposed approach in the second instance of the single-area test system with larger wind power integration.

4.2.1 Instance I

The admissible wind power intervals for instance I of the single-area test system are shown as the shaded regions in Fig. 4.4. The day-ahead solution of the proposed RO approach

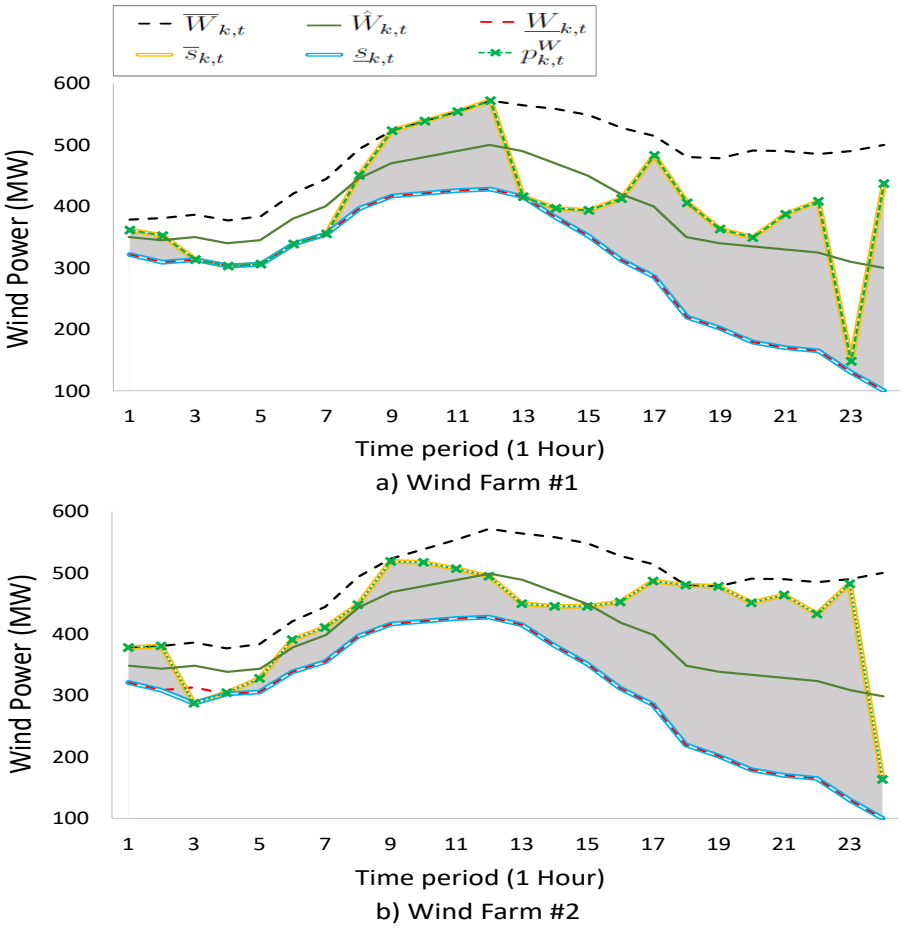

Figure 4.4: Wind power admissible intervals (shaded regions) of the proposed approach

($p^{W}_{k,t}$) with a full budget of uncertainty is also demonstrated in Fig. 4.4. Recall that a full budget of uncertainty corresponds to the case where the output power of all wind farms can have maximum deviations from their predicted values. The four cases of Proposition 2 are observed in Fig. 4.4. For example, case (a) is observed in wind farm #1 output power during periods 9 to 13, where the available wind power can be entirely absorbed. Cases (b) and (c) are observed in wind farm #1 output power during periods 22 and 15, respectively, in which a part of the available wind power cannot be utilized. Case (d) corresponds to

wind farm #2 output power during period 3, where the admissible wind power interval is outside of the uncertainty set.

Recall that the budget of uncertainty in the SCED problem is defined per time period and since there is only one area in this test system, the budget of uncertainty is shown by Γ_t. To demonstrate the effectiveness of the proposed approach, Fig. 4.5 shows the day-ahead wind power utilization versus the budget of uncertainty for two sample time periods (17 and 22), where the admissible intervals correspond to case (b), as shown in Fig. 4.4 . It is observed from Fig. 4.5(a) that, for $\Gamma_{22} \in [0, 0.64]$, the conventional and proposed approaches result in the same wind power utilization, and an increase in the budget of uncertainty leads to higher wind power utilization. This is because the uncertain parameter $\tilde{W}_{k,t}$ of the conventional approach is still within the admissible wind power interval and is equal to the uncertain parameter $\tilde{s}_{k,t}$ of the proposed approach. Thus, since within the admissible wind power interval the problem feasibility is guaranteed, higher budgets of uncertainty corresponds to larger wind power availability interval that consequently results in more wind power utilization without violating the system security.

For $\Gamma_{22} \in (0.64, 1]$, the conventional approach leads to an ineffective budget of uncertainty, and changing the budget of uncertainty does not impact the robust solution and consequently the utilized wind power. The reason is that the uncertain parameter $\tilde{W}_{k,t}$ in the conventional approach is not within the admissible interval ($\tilde{W}_{k,t} \in (\overline{s}_{k,t}, \overline{W}_{k,t}]$), and hence the corresponding constraint becomes redundant, as shown in Section 2.1. In contrast, the proposed robust approach takes this point into account and its uncertain parameter $\tilde{s}_{k,t}$ always lies within the admissible interval. Thus, the proposed approach effectively uses the budget of uncertainty and controls the trade-off between the budget of

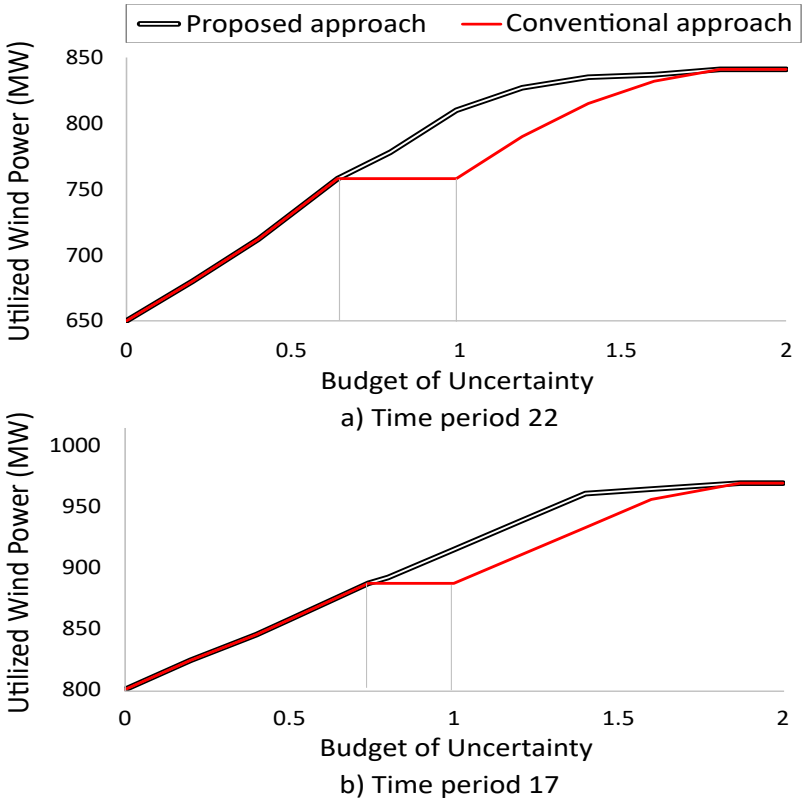

Figure 4.5: Utilized wind power versus budget of uncertainty

uncertainty and wind power utilization, as intuitively expected.

For $\Gamma_{22} \in (1, 2)$, an increase in the budget of uncertainty results in higher wind power utilization in both approaches since the budget of uncertainty is spread out over both wind farms. Finally, for $\Gamma_{22} = 2$ which corresponds to the full budget of uncertainty, both approaches lead to similar overly-conservative solution under the worst-case wind power scenario. Similar observations can be made for time period 17, Fig. 4.5(b) .

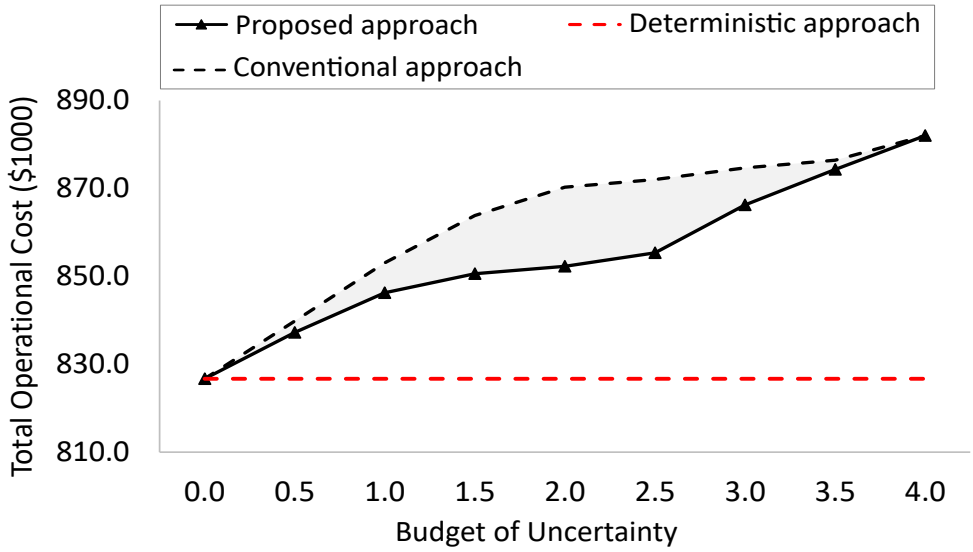

Figure 4.6: Total operational cost under various budgets of uncertainty

4.2.2 Instance II

Fig. 4.6 shows the trade-off between the total operational cost over the 24-hour time horizon and the budget of uncertainty considered for each time period. This trade-off is often referred to as "the price of robustness" (Bertsimas and Sim, 2004) as it indicates the additional operational cost associated with the robust approach to account for uncertainty. Recall that the deterministic approach corresponds to the case where there is no uncertainty, i.e., $\Gamma = 0$. Fig. 4.6 demonstrates that the operational cost goes up as the budget of uncertainty increases since the corresponding solutions become more conservative. A more conservative solution results in more wind power curtailment in critical time periods than can potentially lead to security issues, which in turn increases the objective function due to the wind power curtailment cost (Li et al., 2016a).

The shaded region in Fig. 4.6 demonstrates the effectiveness of the proposed

approach compared to the conventional approach as the budget of uncertainty increases. For $\Gamma = 0$ and $\Gamma = 4$ (full budget of uncertainty), both robust approaches result in similar operational costs. For $0 < \Gamma < 4$, the proposed RO model maps the partially-ineffective budgets into effective budgets and leads to more wind power utilization when the admissible wind power interval is aligned with case (b), as shown in Instance I. Therefore, the proposed approach results in a lower operational cost compared to the conventional approach.

One advantage of the robust approach is that its optimal solution is less sensitive to changes in the uncertain parameter compared to that of the deterministic approach. To demonstrate this advantage, the performance of the robust and deterministic approaches are compared during intra-day optimization, where the actual realization of the uncertain wind power $W_{k,t}^{Actual}$ is considered. For the intra-day optimization, a large number of wind power scenarios are randomly generated within the initial uncertainty set $[\underline{W}_{k,t}, \overline{W}_{k,t}]$. For each scenario, an intra-day SCED problem is solved with $\tilde{W}_{k,t} = W_{k,t}^{Actual}$. The absolute values of the difference between the operational cost of intra-day and day-ahead solutions (ΔC) is calculated. In fact, ΔC represents the weighted sum of the difference between the dispatches in intra-day and day-ahead solutions. This process is repeated until there are up to 100 randomly generated wind power scenarios of $W_{k,t}^{Actual} \in [\hat{W}_{k,t} + r_{k,t}(\underline{W}_{k,t} - \hat{W}_{k,t}), \hat{W}_{k,t} + r_{k,t}(\overline{W}_{k,t} - \hat{W}_{k,t})]$ for values of Γ =1, 2, 3, and 4.

Fig. 4.7 compares the performance of the three approaches in terms of the sensitivity of day-ahead solutions to intra-day solutions where the actual realizations of the uncertain parameter in real-time is known. The deterministic approach corresponds to large ΔC values since its day-ahead solution results in low operational cost, especially low wind power curtailment cost, that considerably differs from the intra-day wind power

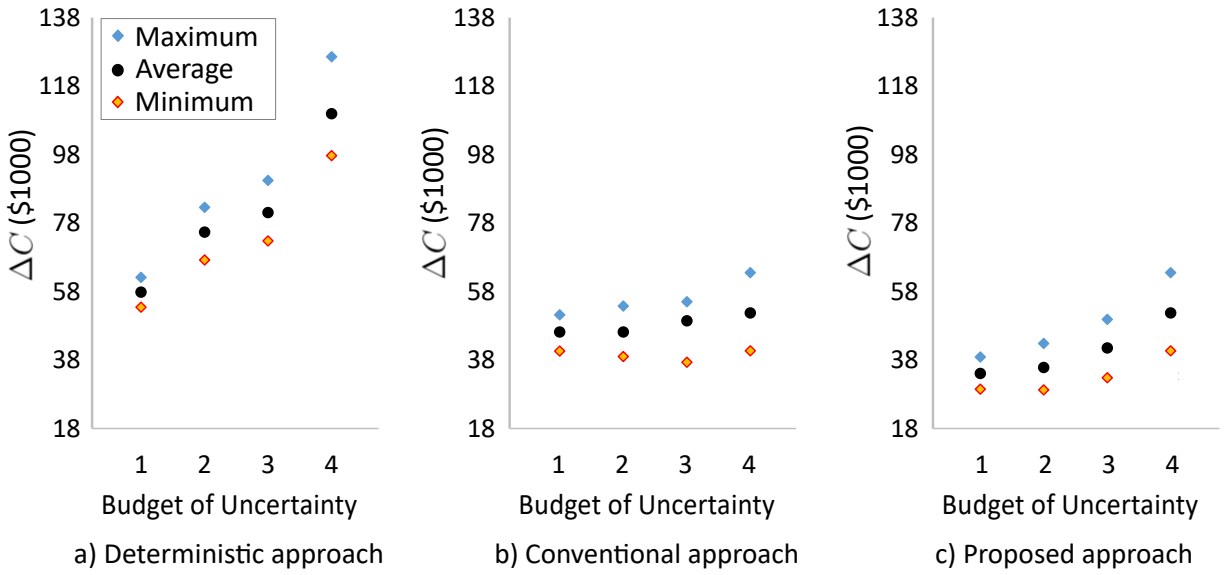

Figure 4.7: The sensitivity of day-ahead solutions to intra-day solutions with respect to the budget of uncertainty

curtailment since the deterministic approach does not take wind power uncertainty into account. The proposed robust approach corresponds to small ΔC values as its day-ahead solution accounts for the worst-case wind power scenario. Particularly, for $\Gamma = 1$, the average ΔC for the proposed robust approach is approximately 25% and 40% less than those of the conventional robust and deterministic approaches, respectively. The smaller ΔC in the proposed approach − compared to the conventional robust approach − is because the proposed approach maps the partially-ineffective budgets of uncertainty to effective budgets of uncertainty and consequently leads to less day-ahead wind power curtailment and provides a day-ahead solution that is closer to the intra-day solution.

4.3 Two-Area Test System

In this section, the performance of the proposed RO approach in the two-area mixed AC-HVDC system is examined from various aspects such as robustness, power transfer controllability, reliability, and sensitivity to system parameters.

4.3.1 Wind Power Generation

Figs. 4.8 demonstrates the admissible wind power interval (shaded regions) obtained from solving the look-ahead SCED optimization problem using the proposed robust approach. The look-ahead wind power dispatches based on the deterministic ($\Gamma_{a,t} = 0$) and robust ($\Gamma_{a,t} = 1$) SCED optimization as well as a sample wind power scenario in real-time (W^{Actual}) are shown in Fig. 4.8. Furthermore, Fig. 4.9 shows the remaining upward reserve (RUR), inadequate upward reserve (IUR), and inadequate downward reserve (IDR) associated with area 2, which are calculated based on the the look-ahead scheduled wind power dispatch ($p^{W}_{k,t}$) and the intra-day optimization for the sample wind power scenario. In particular, if $W^{Actual}_{k,t} < p^{W}_{k,t}$ in the intra-day optimization, UR is required to compensate for the wind power shortage. Otherwise, the system may encounter security issues. RUR is calculated after responding to these shortages and is an indicator of the system security level. IUR corresponds to the additional reserve needed for meeting the system security requirements to respond to contingencies and outages. On the other hand, if $p^{W}_{k,t} \leq W^{Actual}_{k,t}$, wind power curtailment will be required when there is IDR in the system. IDR is not an indicator of system security violation, as opposed to IUR, and corresponds to an extra DR that is required to prevent potential wind power curtailment. The following findings are obtained

from Figs. 4.8 and 4.9 for area 2. Similar conclusion can be made about area 1 as well.

- During time periods 9 and 10, since there is a sudden drop in $\hat{W}_{k,t}$ of area 2, the maximum wind power admissibility ($\overline{s}_{k,t}$) of the look-ahead solution is reduced to guarantee an RUR larger than 400 MW (UR requirement in constraint 3.27) under potential low wind scenarios in the intra-day optimization. However, even though the look-ahead wind power dispatch in the deterministic approach is more during these periods, it is outside of the admissible region and may causes security issues. In particular, RUR based on the proposed approach is above the security baseline over the entire time horizon (IUR= 0), while in the deterministic approach, during critical time periods 9, 14, and 15, the security of the system cannot be guaranteed due to the non-zero IUR under potential low wind power scenarios, such as the sample wind power scenario, in the intra-day optimization.

- During time periods 13 to 16 with low power demand, $\overline{s}_{k,t}$ decreases to ensure that look-ahead $p^W_{k,t}$ resulting from the proposed approach is set at a low level to meet the DR requirement of the system in the intra-day optimization. Thus, as $p^W_{k,t}$ is reduced, conventional generators are dispatched at a high level to accommodate the system DR requirement under potential high wind scenarios in the intra-day optimization.

- The DR requirement in constraint (3.28) is met based on the proposed and deterministic approaches, while the maximum IDR is larger based on the proposed approach for the sample wind power scenario. A higher IDR resulting from the proposed approach does not necessarily result in more intra-day wind power curtailment over the entire time horizon (compared to the deterministic approach) since the intra-day IDR occurs less frequently in the proposed approach.

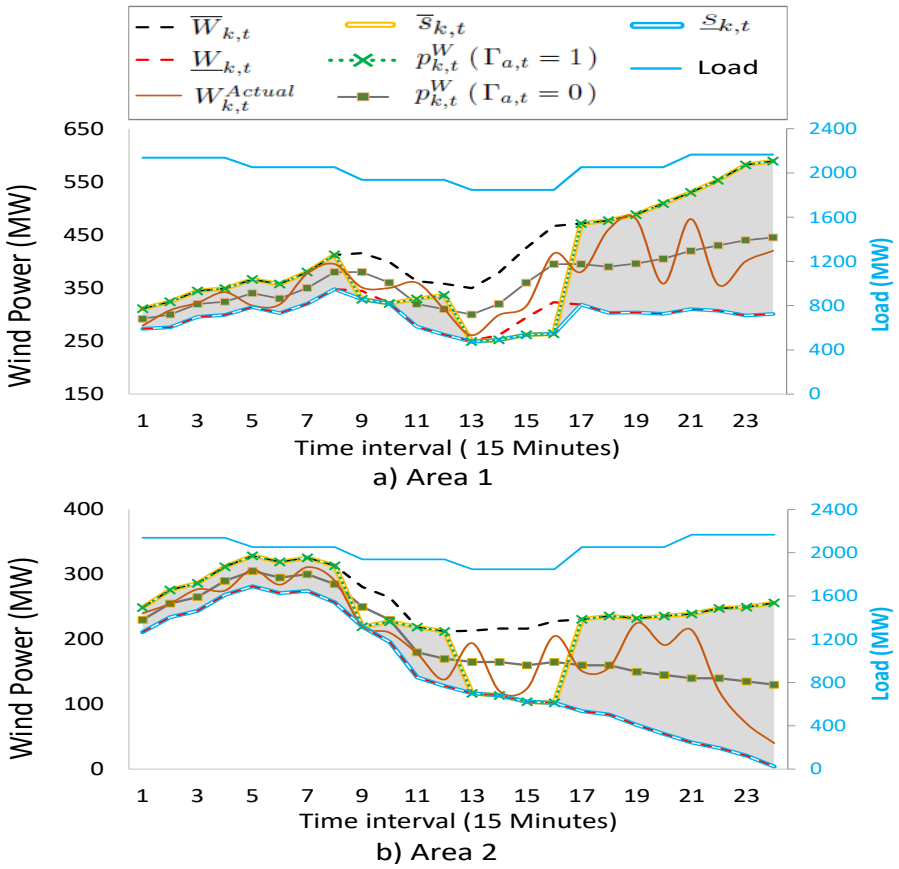

Figure 4.8: Look-ahead power wind power dispatch of the two-area system

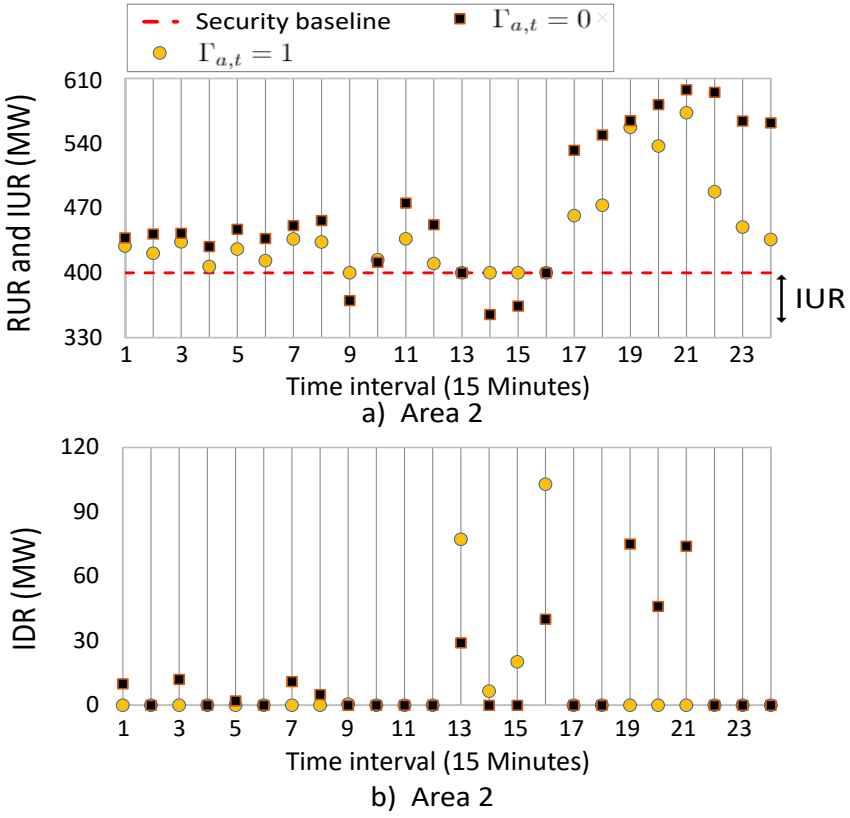

Figure 4.9: RUR, IUR, and IDR over a 6-hour time horizon

Table 4.1: Look-ahead and intra-day solutions of the proposed and deterministic approaches

		Look-ahead			Intra-day (average values)										
								IUR				IDR			
		Curtailed wind	Utilized wind	Operational cost	Curtailed wind	Utilized wind	Operational cost	% of scenarios with IUR during N intervals or more:			Max IUR	% of scenarios with IDR during N intervals or more:			Max IDR
Budget	Area	(MWh)	(MWh)	×($1000)	(MWh)	(MWh)	×($1000)	N=1	N=2	N=3	(MW)	N=6	N=8	N=10	(MW)
$\Gamma_{a,t}=0$	1	94	8,702	2,340.1	639	8,932	2,371.2	97.1	85.3	60.8	51	100	97.6	85.3	132
	2	0	4,870		471	5,021		95.6	79.8	51.1	58	99.5	95.7	83.1	107
$\Gamma_{a,t}=1$	1	814	9,384	2,395.8	703	9,041	2,383.8	0	0	0	0	91.2	19.2	0	189
	2	698	5,649		567	5,281		0	0	0	0	54.3	0	0	121

4.3.2 Reliability Analysis and Robustness Verification

To verify the robustness and reliability of the proposed approach, 1000 wind power scenarios ($W_{k,t}^{Actual}$) are randomly generated, and an intra-day optimization is carried out for each scenario. In the intra-day optimization, the tie-line power flows are set to the flows obtained from the look-ahead solutions. The curtailed wind, utilized wind, operational cost, IUR, and IDR resulting from both approaches are summarized in Table 4.1, where the maximum IUR and IDR are calculated with respect to the look-ahead solution and are obtained from all scenarios over the entire time horizon. The rest of the table corresponds to average values over all scenarios. Table 4.1 shows that the proposed approach outperforms the deterministic approach in terms of satisfying the UR requirement. For example, the solution from the deterministic approach fails to meet the system UR requirement at least during one time interval in approximately 97% of the generated wind power scenarios, while the solution from the proposed approach does not result in a positive IUR. Furthermore, the look-ahead solution of the proposed approach results in less frequent IDR over the time horizon. In Table 4.1, the look-ahead solution of the proposed approach corresponds to a higher wind power utilization and wind power curtailment, compared to the deterministic approach. The reason is that $\Gamma_{a,t} = 1$ corresponds to a larger wind power availability interval and consequently a higher look-ahead wind power utilization when the available

wind power can be dispatched without any security issue (e.g., periods 18-24 of Fig. 4.4). On the other hand, the larger wind power availability interval enables a higher look-ahead wind power curtailment during critical periods (e.g., periods 13-16 of Fig. 4.4) since it accounts for the worst-case scenario to guarantee the system security under all wind power scenarios in real-time. Thus, the worst-case wind curtailment consequently leads to a higher operational cost in the proposed approach. This extra cost is considered as the price of robustness, i.e., the price that is paid for accommodating the system security under wind power uncertainty (Bertsimas and Sim, 2004). For each approach, the intra-day wind power curtailment and operational cost of Table 4.1 correspond to the solution of the intra-day optimization when the tie-line power flows are set to the flows obtained from its look-ahead solution. This point will be more elaborated on in Section 4.4.

4.3.3 Maximum Wind Power Admissibility

To study the impact of line limits on the maximum wind power admissibility $\overline{s}_{k,t}$, the power flow limits of internal lines 18, 20, and 22 in area 1 are decreased and other system settings are kept unchanged. Fig. 4.10(a) shows $\overline{s}_{k,t}$ of area 1 for various power flow limits. A lower power flow limit results in more wind power curtailment to prevent overloading of the lines under high wind power scenarios. In Fig. 4.10(b), the impacts of $R^d_{1,t}$ on $\overline{s}_{k,t}$ of area 1 is illustrated (line flow limits are the original values), where higher values of $R^d_{1,t}$ result in more wind power curtailment to satisfy the DR requirements of the system under all wind power scenarios in real-time. A similar conclusion can be made for $R^u_{1,t}$ that higher values of $R^u_{1,t}$ result in more wind power curtailment to ensure the RUR is sufficient to satisfy UR requirements of the system under all wind power scenarios in real-time.

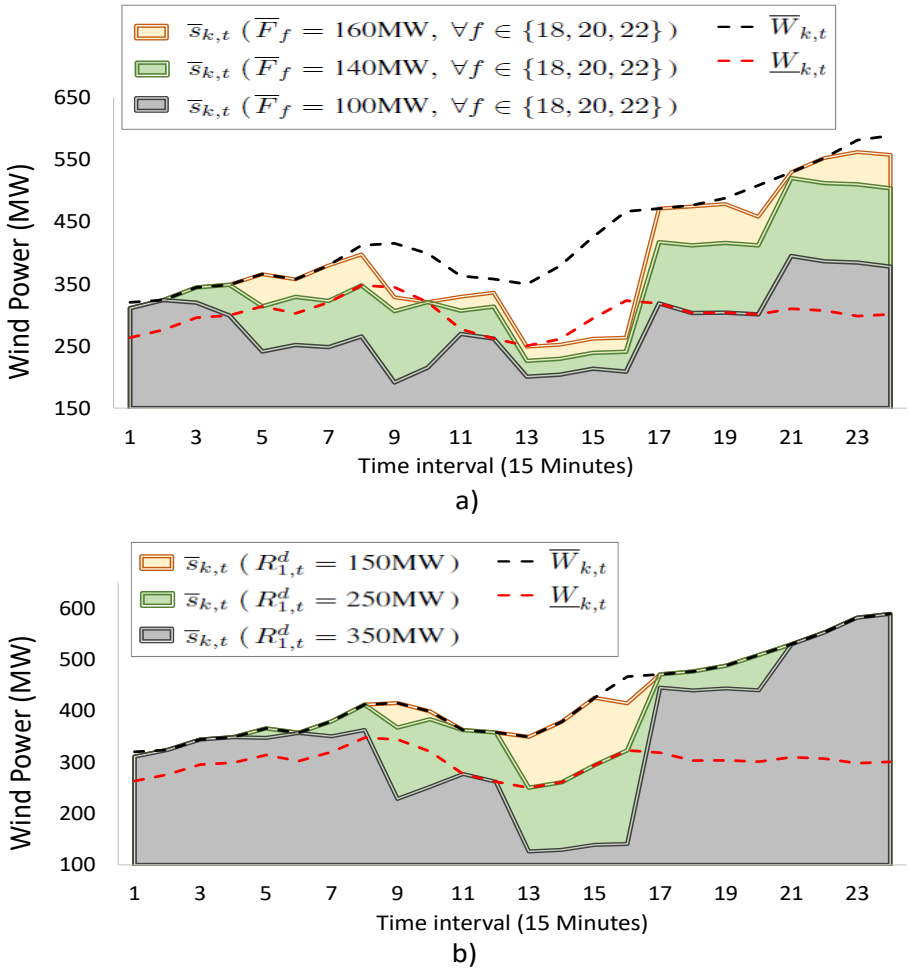

Figure 4.10: Sensitivity of $\overline{s}_{k,t}$ in area 1 to a) $\overline{F}_f$ and b) $R^d_{1,t}$.

4.3.4 System Type

Fig. 4.11 shows the tie-line flows based on the look-ahead RO approach with $\Gamma_{a,t} = 1$ for AC and mixed AC-HVDC systems, where a positive flow denotes power flowing from area 1 to area 2. The AC system is considered as a large single-area system, where the tie-line flows are described in constraint (3.11). Fig. 4.11 shows that in the mixed AC-HVDC

system, the proposed approach more dynamically responds to the variability of wind and load profiles. For example, the proposed approach in the mixed AC-HVDC system results in less power transfer to area 2 during time periods 13-16 due to low wind power in area 1, while in later time periods, the net power exchange of area 1 with the adjacent area increases due to higher levels of wind power in area 1. This is because the tie-line flows in the mixed AC-HVDC system can be independently controlled (modeled as external injections in the optimization problem). However, such a controllability does not exist in the AC system since the power flow in the AC tie-lines is more constrained due to its dependency on the voltage angle of the boundary buses, which is incorporated in $G^I_{f,i}$ in constraint (3.11). Table 4.2 summarizes the look-ahead solution of the proposed approach in both systems and shows that the mixed AC-HVDC system outperforms the AC system in terms of utilized wind power and total operational cost.

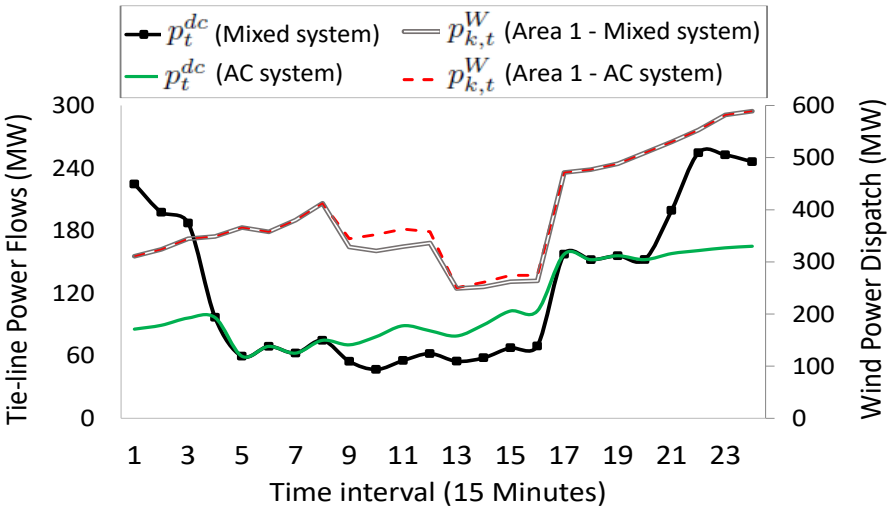

Figure 4.11: Tie-line flows and wind power dispatches of area 1 based on the look-ahead RO approach in AC and mixed AC-HVDC systems for $\Gamma_{a,t} = 1$

Table 4.2: Look-ahead solution of the proposed approach in AC and mixed AC-HVDC systems

System	Power exchange (MWh)	Utilized wind power (MWh)	Total operational cost ($1000)
AC	2,593	14,942	2,403.6
Mixed	3,010	15,033	2,395.8

4.4 Three-Area Test System

Tables 4.3 and 4.4 present the look-ahead solution based on the proposed RO and conventional approaches for AC and mixed AC-HVDC systems under various budgets of uncertainty. The following observations can be obtained for the proposed approach form Tables 4.3 and 4.4:

- Larger budgets of uncertainty result in more conservative solutions (Bertsimas and Sim, 2004), where more wind power is curtailed in the look-ahead solution to ensure the system security under the worst-case wind power scenario in real-time. Thus, as the budget of uncertainty increases, the total operational cost increases due to the increased wind power curtailment cost.

- The total operational cost of the mixed AC-HVDC system is lower than that of the AC system since more wind power is utilized in the entire system due to the controllability of HVDC tie-line power flows.

- The level of conservatism of the solution can be adjusted based on the budget of uncertainty. A larger budget of uncertainty leads to a more conservative solution (higher robustness) with more wind power curtailment and consequently a higher operational cost.

Table 4.3: Look-ahead solution based on the proposed approach for AC and mixed AC-HVDC systems under various budgets of uncertainty

		Mixed system			AC system		
Budgets		Curt. wind	Utilized wind	Operational cost	Curt. wind	Utilized wind	Operational cost
$\Gamma_{3,t}$	$\Gamma_{1,t}$	(MWh)	(MWh)	($1000)	(MWh)	(MWh)	($1000)
0.0	0.0	131	34,447	3,269.7	1,572	33,066	3,338.3
1.0	0.5	901	36,916	3,320.4	2,779	34,146	3,416.5
	1.5	1,453	38,870	3,335.4	4,398	35,925	3,442.9
	3.0	2,343	39,605	3,372.0	5,51	36,797	3,468.9
2.0	0 .5	1,494	38,647	3,339.6	4,348	35,793	3,439.9
	1.5	1,916	39,723	3,353.2	4,888	36,749	3,455.1
	3.0	3,009	40,254	3,402.1	5,850	37,413	3,503.1

Table 4.4: Look-ahead solution based on the conventional robust approach for AC and mixed AC-HVDC systems under various budgets of uncertainty

		Mixed system			AC system		
Budgets		Curt. wind	Utilized wind	Operational cost	Curt. wind	Utilized wind	Operational cost
$\Gamma_{3,t}$	$\Gamma_{1,t}$	(MWh)	(MWh)	($1000)	(MWh)	(MWh)	($1000)
0.0	0.0	131	34,447	3,269.7	1,572	33,066	3,338.3
1.0	0.5	993	36,832	3,325.0	2,835	34,090	3,418.8
	1.5	1,513	38,810	3,338.4	4,424	35,899	3,462.6
	3.0	2,385	39,563	3,376.1	5,237	36,711	3,473.2
2.0	0 .5	1,618	38,523	3,345.8	4,449	35,692	3,443.9
	1.5	2,138	39,501	3,364.3	5,038	36,599	3,462.6
	3.0	3,009	40,254	3,402.1	5,850	37,413	3,503.1

- A larger budget of uncertainty corresponds to a larger wind power availability interval and consequently a solution with larger curtailed and utilized wind power over the entire time horizon. The reason is that a larger wind power availability enables more wind power curtailment to ensure the system security during time periods with potential low wind power dispatch. In contrast, in the rest of time periods, where the wind power can be dispatched at a high level without violating the security of the system, a larger wind power availability interval results in more utilized wind power.

- The proposed approach outperforms the conventional robust approach, in terms of wind power utilization and leads to lower operational costs. The reason is that the proposed approach maps the ineffective budgets into effective budgets, as shown in section 4.2.1. For no and full budgets of uncertainty, both approaches lead to similar solutions, which are shown in the first and the last rows of Tables 4.3 and 4.4, respectively.

In a multi-area power system, power exchanges among areas are scheduled based on the day-ahead or look-ahead market. Changing a scheduled tie-line flow in real-time requires an agreement from all neighbouring areas since such changes may lead to security issues or additional costs. To verify the real-time cost efficiency and reliability of the look-ahead robust solution of the proposed approach, the wind power curtailment and operational cost associated with the intra-day optimization should be calculated. In this section, three strategies are proposed to solve the intra-day optimization problem: i) constant flows (CF), ii) semi-flexible flows (SFF), and iii) flexible flows (FF). In CF, no deviation from the scheduled tie-line flows (based on the look-ahead solution) is allowed. In the SFF, relatively small deviations (5%) from the scheduled tie-line flows are allowed, but a penalty term is added to the objective function to account for the deviations. In FF, unlimited deviations from the scheduled tie-line flows are allowed.

To performe the intra-day optimization model under various strategies, 100 wind power scenarios are generated, and the SCED problem is solved under each generated wind power scenario for AC and mixed AC-HVDC systems. The intra-day solutions based on CF and SFF strategies are summarized in Tables 4.5 and 4.6, respectively. Maximum, average, and minimum values of the total operational cost based on CF, SFF, and FF

strategies as well as the total operational cost of the look-ahead robust and deterministic solutions for the mixed AC-HVDC system are plotted in Fig. 4.12. The following findings can be observed from Tables 4.5 and 4.6 and Fig. 4.12:

- The deterministic approach does not guarantee the system security in real-time as it results in IUR (IUR > 0).
- The intra-day robust solution corresponds to no IUR (IUR $= 0$), and therefore the proposed RO approach guarantees the system security in real-time. However, the intra-day robust solution corresponds to a higher IDR, as compared to the deterministic approach, since more wind power is utilized in the proposed approach, which corresponds to lower power dispatches of conventional generators for a given load. Thus, the robust solution corresponds to a lower DR in the system, which is required to prevent wind power curtailment. In addition, the look-ahead robust solution provides an upper bound for the total operational cost of the intra-day robust solutions since the look-ahead decisions are made for the worst-case wind power scenario.
- The SFF strategy corresponds to a lower total operational cost, compared to the CF strategy, due to its flexibility in adjusting the scheduled tie-line flows. The tie-line flow deviations correspond to the flow difference between the look-ahead and intra-day solutions.
- The FF strategy corresponds to a lower bound for the total operational cost in real-time as in this strategy, the tie-line flows can be fully adjusted based on $W_{k,t}^{Actual}$.
- In the mixed AC-HVDC power system, the wind power utilization and operational cost are respectively higher and lower than those of the AC system, due to the con-

Table 4.5: Intra-day RO solution based on CF strategy

		Mixed AC-HVDC system					AC system				
Budgets		Curtailed wind	Utilized wind	Max IUR	Max IDR	Operational cost	Curtailed wind	Utilized wind	Max IUR	Max IDR	Operational cost
$\Gamma_{3,t}$	$\Gamma_{1,t}$	(MWh)	(MWh)	(MW)	(MW)	×($1000)	(MWh)	(MWh)	(MW)	(MW)	×($1000)
0.0	0.0	544	35,088	131	181	3,333.5	2,532	32,100	212	162	3,447.4
				-				16% of scenarios are infeasible			
	0.5	591	35,055	0	196	3,320.1	2,061	33,585	0	183	3,414.0
1.0	1.5	744	36,895	0	201	3,329.3	3,352	34,290	0	194	3,439.2
	3.0	928	37,849	0	219	3,353.2	3,594	35,283	0	208	3,458.7
	0.5	451	35,419	0	227	3,330.4	3,101	32,769	0	198	3,425.1
2.0	1.5	598	38,025	0	279	3,339.1	3,312	35,412	0	271	3,448.1
	3.0	1,342	38,162	0	282	3,371.9	3,921	35,583	0	273	3,490.3

Table 4.6: Intra-day RO solution based on SFF strategy

		Mixed AC-HVDC system				AC system			
Budgets		Curtailed wind	Utilized wind	Operation cost	Tie-line flow deviations	Curtailed wind	Utilized wind	Operation cost	Tie-line flow deviations
$\Gamma_{3,t}$	$\Gamma_{1,t}$	(MWh)	(MWh)	($1000)	(MWh)	(MWh)	(MWh)	($1000)	(MWh)
0.0	0.0	472	35,161	3,325.6	334	2,395	32,237	3,434.1	206
				-		7% of scenarios are infeasible			
	0.5	301	35,339	3,316.1	531	1,790	33,858	3,403.3	281
1.0	1.5	398	37,233	3,322.9	567	3,305	34,105	3,770.3	286
	3.0	565	38,311	3,337.2	628	3,382	35,495	3,447.2	318
	0.5	331	35,534	3,321.4	683	2,820	32,949	3,414.8	241
2.0	1.5	420	38,303	3,325.1	702	3,130	35,493	3,433.1	294
	3.0	908	38,595	3,351.6	815	3,786	35,717	3,466.7	335

trallability of HVDC tie-line flows. However, in the AC system, the IDR is relatively smaller due to lower tie-line flows. The lower power transfer from area 1 (generation-dominant area) to the other areas results in higher dispatch levels of conventional generators of areas 2 and 3. This ultimately spares more DR in areas 2 and 3 of the AC system and corresponds to a lower IDR in real-time.

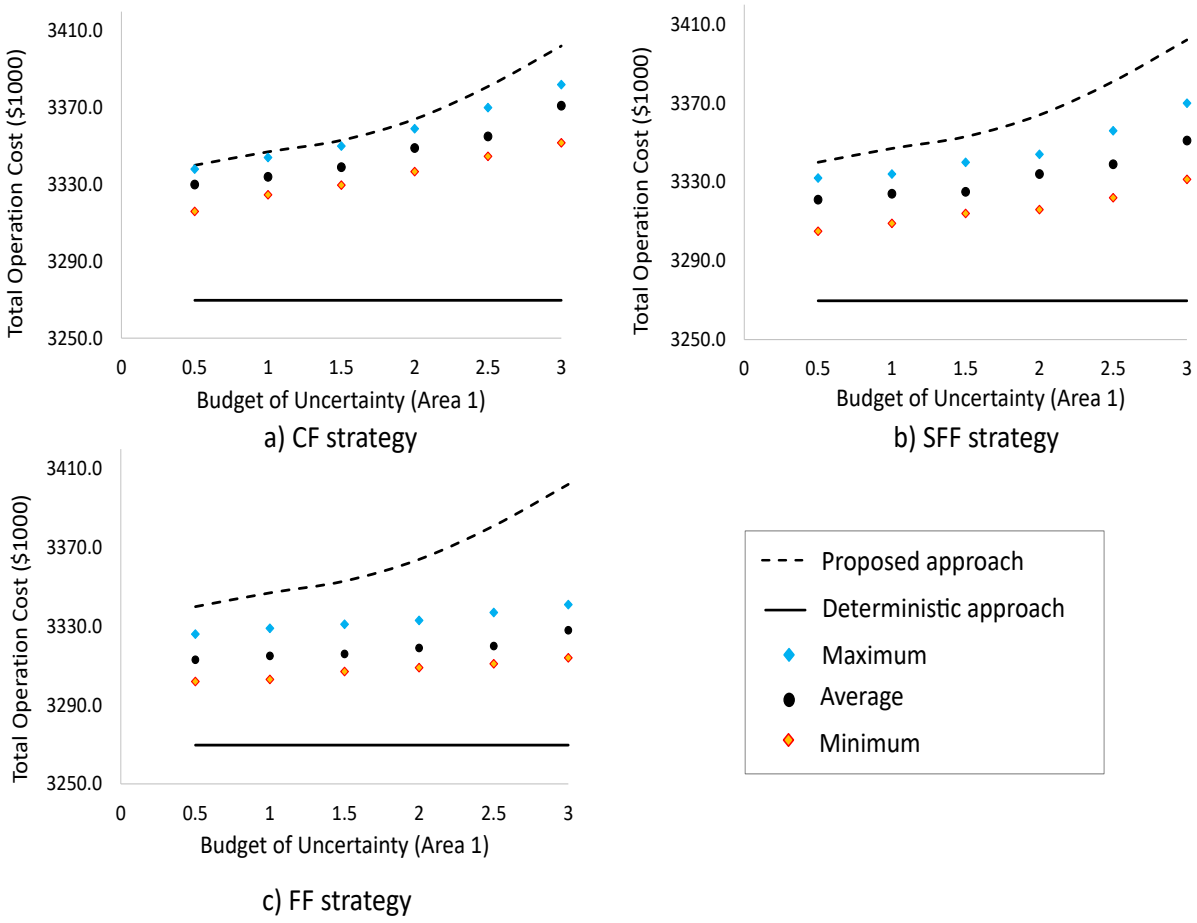

Figure 4.12: Maximum, average, and minimum values of the total operational cost based on the intra-day robust, look-ahead robust, and look-ahead deterministic approaches ($\Gamma_{3,t} = 2$)

Chapter 5

Conclusion

The development of robust optimization (RO) models is essential to address wind power uncertainty in the security-constrained economic dispatch (SCED) problem for alternating current (AC)-high voltage direct current (HVDC) power systems. In such SCED problems, available wind power is often used in the right-hand side (RHS) of the constraint associated with the upper bound of wind power dispatch. The traditional RO approach for solving such SCED problems may be overly conservative since it finds a solution that is feasible under any possible realization of the uncertain wind power. The budget of uncertainty approach has been proposed in the literature of RO to adjust the level of conservatism. This thesis showed that the conventional budget of uncertainty approach is not particularly meaningful for a class of problems with the RHS uncertainty since increasing the budget of uncertainty may not always impact the the level of conservatism of the robust solutions. Therefore, any consideration of the budget of uncertainty beyond a certain threshold would lead to "partially-ineffective" budgets.

This thesis proposed a new two-stage RO approach to tackle the uncertainty in problems with RHS uncertainty. The proposed two-stage approach first solves an auxiliary problem to identify an admissible uncertainty set within which the feasibility of the solution is guaranteed. Then, an effective uncertainty set is defined as a subset of the admissible set where the worst-case scenario always occurs. In the second stage, an uncertainty budget is incorporated in the model by mapping the partially-ineffective budgets into effective budgets. This thesis showed that the proposed model not only effectively controls the level of conservatism in such problems, but also provides meaningful insights into the trade-off between the robustness and operational cost.

The applicability of the proposed approach was examined for the SCED problem in mixed AC-HVDC multi-area power systems. This thesis considered the new advancements in multi-area power systems, where HVDC transmission lines are used to transfer power from offshore wind farms to onshore loads, and addressed the operating characteristics and reliability requirements of such mixed AC-HVDC systems. The existing gaps in the literature of robust SCED were addressed by considering the impact of wind power curtailment on the operational cost and reliability requirements of the system. Finally, the practical merits of the proposed approach from various aspects such as reliability, robustness, and cost efficiency were demonstrated.

Power dispatch problems, in particular the SCED problem, are only one of the many areas dealing with the RHS uncertainty. In many real-world applications such as project management, scheduling, dynamic inventory management, and telecommunication problems, various parameters − such as time, resource availability, stock level, arrival rates − appear in the RHS of constraints which are potentially uncertain. The proposed

approach can be adapted in such problem settings to effectively control the level of conservatism of the robust solutions.

Bibliography

Aguado, J. A., Quintana, V. H., and Conejo, A. J. (1999). Optimal power flows of interconnected power systems. In *Power Engineering Society Summer Meeting, 1999. IEEE*, volume 2, pages 814–819. IEEE.

Ahmadi-Khatir, A., Conejo, A. J., and Cherkaoui, R. (2013). Multi-area energy and reserve dispatch under wind uncertainty and equipment failures. *IEEE Transactions on Power Systems*, 28(4):4373–4383.

Ahmadi-Khatir, A., Conejo, A. J., and Cherkaoui, R. (2014). Multi-area unit scheduling and reserve allocation under wind power uncertainty. *IEEE Transactions on Power Systems*, 29(4):1701–1710.

Al Farsi, F., Albadi, M., Hosseinzadeh, N., and Al Badi, A. (2015). Economic dispatch in power systems. In *GCC Conference and Exhibition (GCCCE), 2015 IEEE 8th*, pages 1–6. IEEE.

Amelin, M. (2009). Comparison of capacity credit calculation methods for conventional power plants and wind power. *IEEE Transactions on Power Systems*, 24(2):685–691.

Ang, M., Lim, Y. F., and Sim, M. (2012). Robust storage assignment in unit-load warehouses. *Management Science*, 58(11):2114–2130.

Anstine, L., Burke, R., Casey, J., Holgate, R., John, R., and Stewart, H. (1963). Application of probability methods to the determination of spinning reserve requirements for the Pennsylvania-New jersey-Maryland interconnection. *IEEE Transactions on Power Apparatus and Systems*, 82(68):726–735.

Atamtürk, A. and Zhang, M. (2007). Two-stage robust network flow and design under demand uncertainty. *Operations Research*, 55(4):662–673.

Bakirtzis, A. G. and Biskas, P. N. (2003). A decentralized solution to the DC-OPF of interconnected power systems. *IEEE Transactions on Power Systems*, 18(3):1007–1013.

Baldick, R., Kim, B. H., Chase, C., and Luo, Y. (1999). A fast distributed implementation of optimal power flow. *IEEE Transactions on Power Systems*, 14(3):858–864.

Baradar, M., Ghandhari, M., Van Hertem, D., and Kargarian, A. (2012). Power flow calculation of hybrid AC/DC power systems. In *Power and Energy Society General Meeting, 2012 IEEE*, pages 1–6. IEEE.

Ben-Tal, A., El Ghaoui, L., and Nemirovski, A. (2009). *Robust optimization*, volume 28. Princeton University Press.

Ben-Tal, A. and Nemirovski, A. (1998). Robust convex optimization. *Mathematics of operations research*, 23(4):769–805.

Ben-Tal, A. and Nemirovski, A. (1999). Robust solutions of uncertain linear programs. *Operations research letters*, 25(1):1–13.

Ben-Tal, A. and Nemirovski, A. (2000). Robust solutions of linear programming problems contaminated with uncertain data. *Mathematical programming*, 88(3):411–424.

Ben-Tal, A. and Nemirovski, A. (2002). Robust optimization–methodology and applications. *Mathematical Programming*, 92(3):453–480.

Ben-Tal, A. and Nemirovski, A. (2008). Selected topics in robust convex optimization. *Mathematical Programming*, 112(1):125–158.

Bertsimas, D., Brown, D. B., and Caramanis, C. (2011). Theory and applications of robust optimization. *SIAM review*, 53(3):464–501.

Bertsimas, D., Litvinov, E., Sun, X. A., Zhao, J., and Zheng, T. (2013). Adaptive robust optimization for the security constrained unit commitment problem. *IEEE Transactions on Power Systems*, 28(1):52–63.

Bertsimas, D. and Sim, M. (2003). Robust discrete optimization and network flows. *Mathematical programming*, 98(1-3):49–71.

Bertsimas, D. and Sim, M. (2004). The price of robustness. *Operations research*, 52(1):35–53.

Bertsimas, D. and Thiele, A. (2004). A robust optimization approach to supply chain management. In *International Conference on Integer Programming and Combinatorial Optimization*, pages 86–100. Springer.

Bertsimas, D. and Thiele, A. (2006). A robust optimization approach to inventory theory. *Operations research*, 54(1):150–168.

Billinton, R. and Bollinger, K. E. (1968). Transmission system reliability evaluation using Markov processes. *IEEE Transactions on power apparatus and systems*, (2):538–547.

Billinton, R. and Fotuhi-Firuzabad, M. (2000). A reliability framework for generating unit commitment. *Electric Power Systems Research*, 56(1):81–88.

Billinton, R. and Karki, R. (1999). Capacity reserve assessment using system well-being analysis. *IEEE Transactions on Power Systems*, 14(2):433–438.

Birge, J. R. and Louveaux, F. (2011). *Introduction to stochastic programming*. Springer Science & Business Media.

Biskas, P. and Bakirtzis, A. (2005). A decentralized solution to the security constrained DC-OPF problem of multi-area power systems. In *Power Tech, 2005 IEEE Russia*, pages 1–7. IEEE.

Biskas, P. and Bakirtzis, A. (2006). Decentralised OPF of large multiarea power systems. *IEE Proceedings-Generation, Transmission and Distribution*, 153(1):99–105.

Chan, T. C., Mahmoudzadeh, H., and Purdie, T. G. (2014). A robust-CVaR optimization approach with application to breast cancer therapy. *European Journal of Operational Research*, 238(3):876–885.

Chang, Y.-C., Yang, W.-T., and Liu, C.-C. (1993). Improvements on the line outage distribution factor for power system security analysis. *Electric power systems research*, 26(3):231–236.

Chen, C.-L., Chen, Z.-Y., and Lee, T.-Y. (2014). Multi-area economic generation and reserve dispatch considering large-scale integration of wind power. *International Journal of Electrical Power & Energy Systems*, 55:171–178.

Chowdhury, B. H. and Rahman, S. (1990). A review of recent advances in economic dispatch. *IEEE Transactions on Power Systems*, 5(4):1248–1259.

Chu, M., Zinchenko, Y., Henderson, S. G., and Sharpe, M. B. (2005). Robust optimization for intensity modulated radiation therapy treatment planning under uncertainty. *Physics in Medicine & Biology*, 50(23):5463.

Cohn, N. (1956). Some aspects of tie-line bias control on interconnected power systems. *Transactions of the American Institute of Electrical Engineers. Part III: Power Apparatus and Systems*, 75(3):1415–1436.

Conejo, A. J. and Aguado, J. A. (1998). Multi-area coordinated decentralized DC optimal power flow. *IEEE Transactions on Power Systems*, 13(4):1272–1278.

Di Placido, A. M., Pressnail, K. D., and Touchie, M. F. (2014). Exceeding the ontario building code for low-rise residential buildings: Economic and environmental implications. *Building and Environment*, 77:40–49.

Ding, T., Lv, J., Bo, R., Bie, Z., and Li, F. (2016). Lift-and-project MVEE based convex hull for robust SCED with wind power integration using historical data-driven modeling approach. *Renewable energy*, 92:415–427.

Duggal, I. (2012). AC-DC microgrid optimal power flow.

El Ghaoui, L. and Lebret, H. (1997). Robust solutions to least-squares problems with uncertain data. *SIAM Journal on matrix analysis and applications*, 18(4):1035–1064.

Falk, J. E. (1976). Exact solutions of inexact linear programs. *Operations Research*, 24(4):783–787.

Frank, S. and Rebennack, S. (2016). An introduction to optimal power flow: Theory, formulation, and examples. *IIE Transactions*, 48(12):1172–1197.

Frank, S., Steponavice, I., and Rebennack, S. (2012). Optimal power flow: a bibliographic survey I. *Energy Systems*, 3(3):221–258.

Gabrel, V., Murat, C., and Thiele, A. (2014). Recent advances in robust optimization: An overview. *European journal of operational research*, 235(3):471–483.

Goh, J. and Sim, M. (2011). Robust optimization made easy with ROME. *Operations Research*, 59(4):973–985.

Goldfarb, D. and Iyengar, G. (2003). Robust portfolio selection problems. *Mathematics of operations research*, 28(1):1–38.

Gooi, H., Mendes, D., Bell, K., and Kirschen, D. (1999). Optimal scheduling of spinning reserve. *IEEE Transactions on Power Systems*, 14(4):1485–1492.

Grigg, C., Wong, P., Albrecht, P., Allan, R., Bhavaraju, M., Billinton, R., Chen, Q., Fong, C., Haddad, S., Kuruganty, S., et al. (1999). The IEEE reliability test system-1996. a report prepared by the reliability test system task force of the application of probability methods subcommittee. *IEEE Transactions on power systems*, 14(3):1010–1020.

Guan, Y. and Wang, J. (2014). Uncertainty sets for robust unit commitment. *IEEE Transactions on Power Systems*, 29(3):1439–1440.

Hassan, H. and Mohamed, Y. (2014). Market-oriented energy management of a hybrid power system via model predictive control with constraints optimizer. In *PES General Meeting— Conference & Exposition, 2014 IEEE*, pages 1–5. IEEE.

Hassanzadeh, F., Nemati, H., and Sun, M. (2014). Robust optimization for interactive multiobjective programming with imprecise information applied to R&D project portfolio selection. *European Journal of Operational Research*, 238(1):41–53.

Hobbs, B. F., Rothkopf, M. H., O'Neill, R. P., and Chao, H.-p. (2006). *The next generation of electric power unit commitment models*, volume 36. Springer Science & Business Media.

Horn, R. A. (1990). The hadamard product. In *Proc. Symp. Appl. Math*, volume 40, pages 87–169.

Iggland, E., Wiget, R., Chatzivasileiadis, S., and Anderson, G. (2015). Multi-area DC-OPF for HVAC and HVDC grids. *IEEE Transactions on Power Systems*, 30(5):2450–2459.

Jabr, R. A. (2013). Adjustable robust OPF with renewable energy sources. *IEEE Transactions on Power Systems*, 28(4):4742–4751.

Jiang, R., Wang, J., and Guan, Y. (2012). Robust unit commitment with wind power and pumped storage hydro. *IEEE Transactions on Power Systems*, 27(2):800–810.

Jiang, R., Wang, J., Zhang, M., and Guan, Y. (2013). Two-stage minimax regret robust unit commitment. *IEEE Transactions on Power Systems*, 28(3):2271–2282.

Kim, C.-K., Sood, V. K., Jang, G.-S., Lim, S.-J., and Lee, S.-J. (2009). *HVDC transmission: power conversion applications in power systems*. John Wiley & Sons.

Kumar, C. and Alwarsamy, T. (2011). Dynamic economic dispatch–a review of solution methodologies. *European Journal of Scientific Research*, 64(4):517–537.

Kundur, P., Balu, N. J., and Lauby, M. G. (1994). *Power system stability and control*, volume 7. McGraw-hill New York.

Kundur, P., Paserba, J., Ajjarapu, V., Andersson, G., Bose, A., Canizares, C., Hatziargyriou, N., Hill, D., Stankovic, A., Taylor, C., et al. (2004). Definition and classification of power system stability. *IEEE transactions on Power Systems*, 19(2):1387–1401.

Li, Y. and Flynn, P. C. (2004). Deregulated power prices: comparison of volatility. *Energy Policy*, 32(14):1591–1601.

Li, Z., Shahidehpour, M., Wu, W., Zeng, B., Zhang, B., and Zheng, W. (2015a). Decentralized multiarea robust generation unit and tie-line scheduling under wind power uncertainty. *IEEE Transactions on Sustainable Energy*, 6(4):1377–1388.

Li, Z., Wu, W., Shahidehpour, M., and Zhang, B. (2016a). Adaptive robust tie-line scheduling considering wind power uncertainty for interconnected power systems. *IEEE Transactions on Power Systems*, 31(4):2701–2713.

Li, Z., Wu, W., Zhang, B., and Wang, B. (2015b). Robust look-ahead power dispatch with adjustable conservativeness accommodating significant wind power integration. *IEEE Transactions on Sustainable Energy*, 6(3):781–790.

Li, Z., Wu, W., Zhang, B., and Wang, B. (2016b). Decentralized multi-area dynamic economic dispatch using modified generalized benders decomposition. *IEEE Transactions on Power Systems*, 31(1):526–538.

Li, Z., Wu, W., Zhang, B., Wang, B., and Sun, H. (2013). Dynamic economic dispatch with spinning reserve constraints considering wind power integration. In *Power and Energy Society General Meeting (PES), 2013 IEEE*, pages 1–5. IEEE.

Lieu, K.-L., Liu, C.-C., and Chu, R. (1995). Tie line utilization during power system restoration. *IEEE Transactions on Power Systems*, 10(1):192–199.

Lopez, A., Roberts, B., Heimiller, D., Blair, N., and Porro, G. (2012). US renewable energy technical potentials: a GIS-based analysis. Technical report, NREL.

Lorca, A. and Sun, X. A. (2015). Adaptive robust optimization with dynamic uncertainty sets for multi-period economic dispatch under significant wind. *IEEE Transactions on Power Systems*, 30(4):1702–1713.

Lorca, A. and Sun, X. A. (2017). Multistage robust unit commitment with dynamic uncertainty sets and energy storage. *IEEE Transactions on Power Systems*, 32(3):1678–1688.

Lotfjou, A., Shahidehpour, M., Fu, Y., and Li, Z. (2010). Security-constrained unit commitment with AC/DC transmission systems. *IEEE Transactions on power systems*, 25(1):531–542.

Louca, R. and Bitar, E. (2017). Robust AC optimal power flow. *arXiv preprint arXiv:1706.09019*.

Lu, X., Chan, K. W., Xia, S., Zhou, B., and Luo, X. (2018). Security-constrained multi-period economic dispatch with renewable energy utilizing distributionally robust optimization. *IEEE Transactions on Sustainable Energy*.

Lund, H. (2010). The implementation of renewable energy systems. Lessons learned from the Danish case. *Energy*, 35(10):4003–4009.

Mauricio, G. E., Rider, M. J., Mantovani, J., and Shahidehpour, M. (2010). Decentralized AC power flow for real-time multi-TSO power system operation. In *Power and Energy Society General Meeting, 2010 IEEE*, pages 1–7. IEEE.

Mešanović, A., Münz, U., and Ebenbauer, C. (2018). Robust optimal power flow for mixed AC/DC transmission systems with volatile renewables. *IEEE Transactions on Power Systems*, 33(5):5171–5182.

Minoux, M. (2008). Robust linear programming with right-hand-side uncertainty, duality and applications. In *Encyclopedia of Optimization*, pages 3317–3327. Springer.

Minoux, M. (2009). *Robust linear programming with right-hand-side uncertainty, duality and applications*, pages 3317–3327. Springer US, Boston, MA.

Minoux, M. (2012). Two-stage robust LP with ellipsoidal right-hand side uncertainty is NP-hard. *Optimization Letters*, 6(7):1463–1475.

Morales-España, G. (2014). *Unit commitment: computational performance, system representation and wind uncertainty management*. PhD thesis, Comillas Pontifical University.

Nogales, F., Prieto, F., and Conejo, A. (1999). Multi-area AC optimal power flow: A new decomposition approach. In *Proceedings of the 13th Power Systems Control Conference (PSCC)*, pages 1201–1206.

Ouorou, A. (2016). Robust models for linear programming with uncertain right hand side. *Networks*, 68(3):200–211.

Panciatici, P., Hassaine, Y., Fliscounakis, S., Platbrood, L., Ortega-Vazquez, M., Martinez-Ramos, J., and Wehenkel, L. (2010). Security management under uncertainty: from day-ahead planning to intraday operation. In *Bulk Power System Dynamics and Control (iREP)-VIII (iREP), 2010 iREP Symposium*, pages 1–8. IEEE.

Poola, D., Garg, S. K., Buyya, R., Yang, Y., and Ramamohanarao, K. (2014). Robust scheduling of scientific workflows with deadline and budget constraints in clouds. In *2014 IEEE 28th international conference on advanced information networking and applications*, pages 858–865. IEEE.

Ruiz, P. A., Philbrick, C. R., Zak, E., Cheung, K. W., and Sauer, P. W. (2009). Uncertainty management in the unit commitment problem. *IEEE Transactions on Power Systems*, 24(2):642–651.

Saravanan, B., Das, S., Sikri, S., and Kothari, D. (2013). A solution to the unit commitment problem–a review. *Frontiers in Energy*, 7(2):223.

Shahidehpour, M., Yamin, H., and Li, Z. (2003). *Market operations in electric power systems: forecasting, scheduling, and risk management*. John Wiley & Sons.

Shi, D. (2012). *Power system network reduction for engineering and economic analysis*. Arizona State University.

Sim, M. (2004). *Robust optimization*. PhD thesis, Massachusetts Institute of Technology.

Singh, C. (1982). Convex programming with set-inclusive constraints and its applications to generalized linear and fractional programming. *Journal of Optimization Theory and Applications*, 38(1):33–42.

Smith, J. C., Milligan, M. R., DeMeo, E. A., and Parsons, B. (2007). Utility wind integration and operating impact state of the art. *IEEE transactions on power systems*, 22(3):900–908.

Soyster, A. L. (1973). Convex programming with set-inclusive constraints and applications to inexact linear programming. *Operations research*, 21(5):1154–1157.

Stott, B., Alsac, O., and Monticelli, A. J. (1987). Security analysis and optimization. *Proceedings of the IEEE*, 75(12):1623–1644.

Sun, D., Zhang, L., Su, D., and Yuan, Y. (2017). Two-stage robust security-constrained unit commitment with optimizable interval of uncertain wind power output. *Mathematical Problems in Engineering*, 2017.

Vairaktarakis, G. L. (2000). Robust multi-item newsboy models with a budget constraint. *International Journal of Production Economics*, 66(3):213–226.

Van den Bergh, K. and Delarue, E. (2015). An improved method to calculate generation shift keys. Technical report.

Vrakopoulou, M., Margellos, K., Lygeros, J., and Andersson, G. (2013). Probabilistic guarantees for the N-1 security of systems with wind power generation. In *Reliability and Risk Evaluation of Wind Integrated Power Systems*, pages 59–73. Springer.

Wang, C., Liu, F., Wang, J., Wei, W., and Mei, S. (2016). Risk-based admissibility assessment of wind generation integrated into a bulk power system. *IEEE Transactions on Sustainable Energy*, 7(1):325–336.

Wang, J., Shahidehpour, M., and Li, Z. (2008). Security-constrained unit commitment with volatile wind power generation. *IEEE Transactions on Power Systems*, 23(3):1319–1327.

Wiget, R. and Andersson, G. (2012). Optimal power flow for combined AC and multi-terminal HVDC grids based on VSC converters. In *Power and Energy Society General Meeting, 2012 IEEE*, pages 1–8. IEEE.

Wiget, R. and Andersson, G. (2013). DC optimal power flow including HVDC grids. In *Electrical Power & Energy Conference (EPEC), 2013 IEEE*, pages 1–6. IEEE.

Wiget, R., Vrakopoulou, M., and Andersson, G. (2014). Probabilistic security constrained optimal power flow for a mixed HVAC and HVDC grid with stochastic infeed. In *Power Systems Computation Conference (PSCC), 2014*, pages 1–7. IEEE.

Wu, F. F. and Monticelli, A. (1983). Critical review of external network modelling for online security analysis. *International Journal of Electrical Power & Energy Systems*, 5(4):222–235.

Wu, W., Chen, J., Zhang, B., and Sun, H. (2014). A robust wind power optimization method for look-ahead power dispatch. *IEEE Transactions on Sustainable Energy*, 5(2):507–515.

Xie, L., Gu, Y., Zhu, X., and Genton, M. G. (2014). Short-term spatio-temporal wind power forecast in robust look-ahead power system dispatch. *IEEE Transactions on Smart Grid*, 5(1):511–520.

Ye, H. and Li, Z. (2016). Robust security-constrained unit commitment and dispatch with recourse cost requirement. *IEEE Transactions on Power Systems*, 31(5):3527–3536.

Zhang, Z., Chen, Y., Liu, X., and Wang, W. (2019). Two-stage robust security-constrained unit commitment model considering time autocorrelation of wind/load prediction error and outage contingency probability of unit. *IEEE Access*.

Zhao, C., Wang, J., Watson, J.-P., and Guan, Y. (2013). Multi-stage robust unit commitment considering wind and demand response uncertainties. *IEEE Transactions on Power Systems*, 28(3):2708–2717.

Zhao, L. and Zeng, B. (2012). Robust unit commitment problem with demand response and wind energy. In *Power and Energy Society General Meeting, 2012 IEEE*, pages 1–8. IEEE.

Zhu, J. (2015). *Optimization of power system operation*, volume 47. John Wiley & Sons.

Zugno, M. and Conejo, A. J. (2015). A robust optimization approach to energy and reserve dispatch in electricity markets. *European Journal of Operational Research*, 247(2):659–671.